# CENTENNIAL FEATURE ARTICLE

## Theoretical and Computational Studies of Non-RRKM Unimolecular Dynamics†

**Upakarasamy Lourderaj and William L. Hase***

*Department of Chemistry and Biochemistry, Texas Tech University, Lubbock, Texas 79409-1061*

*Received: July 27, 2008; Revised Manuscript Received: December 5, 2008*

A survey is presented of theoretical models and computational studies for unimolecular reaction dynamics. Intrinsic RRKM and non-RRKM dynamics are described, and properties of the unimolecular reactant's classical phase space giving rise to these dynamics are discussed. Quantum dynamical calculations of isolated resonances and state-specific decomposition are reviewed, and the resulting possible mode-specific or statistical state-specific decomposition is delineated. The relationship between the latter and RRKM theory is described. Computational studies give the probability that a molecule dissociates in a time interval of $t \rightarrow t + dt$, that is, the lifetime distribution $P(t)$, and determining unimolecular rate constants versus pressure, energy, and temperature from $P(t)$ is outlined. Non-RRKM behavior evident in $P(t)$ is not always present in the rate constants. The need to include anharmonicity and the proper treatment of the $K$ quantum number, in calculating the RRKM unimolecular rate constant, is explained. The possibility of observing "steps" in unimolecular rate constants is considered. The extensive experimental non-RRKM dynamics found for several classes of chemical reactions are surveyed. The direct coupling of chemical dynamics with electronic structure theory, that is, direct dynamics, has allowed one to study the atomic-level dynamics for numerous unimolecular reactions, and extensive non-RRKM and nonintrinsic reaction coordinate (IRC) dynamics have been discovered. These dynamics for $OH^- + CH_3F$ and $F^- + CH_3OOH$ are reviewed.

### I. Introduction

The research field of unimolecular kinetics and dynamics includes studies of methods for energizing molecules,[1,2] collisional stabilization of vibrationally and rotationally excited molecules,[3−8] product energy partitioning,[9−13] the dynamics of intramolecular vibrational energy redistribution (IVR),[12,14−16] and models for unimolecular decomposition.[17−19] Though each of these topics is of much importance, it is the latter two, which are fundamental to the theory of unimolecular reaction dynamics,[12,17−19] that are considered here. An accurate theory of unimolecular dynamics and kinetics is needed to model unimolecular reactions for many different chemical processes, including atmospheric and combustion chemistry,[20−22] peptide fragmentation,[23−25] dissociation of clusters,[26,27] and ion−molecule reactions.[28−30]

A limiting and widely used model of unimolecular kinetics is the Rice−Ramsperger−Kassel−Marcus (RRKM) theory. This theory is based on the fundamental assumption that a microcanonical ensemble of states exists initially for the energized molecule A* and is then maintained as it decomposes.[12,17−19] Maintaining the microcanonical ensemble, during the unimolecular decomposition, requires rapid and complete IVR among the degrees of freedom of the energized molecule. Details of this theory were developed nearly simultaneously by two groups in the early 1950s,[31−33] while such a microcanonical model for unimolecular dissociation was described somewhat earlier.[34,35] In the ion−molecule community, this microcanonical theory became known as the quasi-equilibrium theory (QET).[33] The Rabinovitch research group was instrumental in initiating and facilitating widespread applications of RRKM theory to interpret experiments.[36−38]

The RRKM/QET rate constant for total energy $E$ and angular momentum $J$ is expressed as

$$k(E,J) = \frac{N^{\ddagger}(E - E_o, J)}{h\rho(E,J)} \quad (1)$$

where $N^{\ddagger}(E - E_o,J)$ is the transition state's sum of states, $\rho(E,J)$ is the unimolecular reactant's density of states, and $E_o$ is the unimolecular threshold. RRKM theory is viewed as a statistical theory since the rate constant is calculated from statistical mechanical properties, and an understanding of the actual dissociation dynamics is unnecessary. The sum and densities of states in eq 1 are calculated for the active degrees of freedom, for which IVR is rapid. Within the framework of RRKM theory, there is the possibility that some modes are not active but are adiabatic and stay in fixed quantum states **n** during the reaction.[32] For this situation, eq 1 becomes

$$k(E,J,\mathbf{n}) = \frac{N^{\ddagger}(E - E_o, J, \mathbf{n})}{h\rho(E,J,\mathbf{n})} \quad (2)$$

A specific degree of freedom which has received considerable interest, regarding its activity or adiabaticity, is the one associated with the $K$ rotational quantum number.[39] An example

† 2008 marked the Centennial of the American Chemical Society's Division of Physical Chemistry. To celebrate and to highlight the field of physical chemistry from both historical and future perspectives, *The Journal of Physical Chemistry* is publishing a special series of Centennial Feature Articles. These articles are invited contributions from current and former officers and members of the Physical Chemistry Division Executive Committee and from *J. Phys. Chem.* Senior Editors.

* To whom correspondence should be addressed.

10.1021/jp806659f CCC: $40.75 
Published on Web 02/25/2009

**Upakarasamy Lourderaj** was born in Pondicherry, India, in 1974. He received his B.Sc. in Chemistry from Tagore Arts College (Pondicherry University, India) in 1995 and M.Sc. in Chemistry from St. Joseph's College (Bharathidasan University, India) in 1998. Later, he obtained his Ph.D. in Chemistry from the Indian Institute of Technology−Kanpur, India, in 2004. He then joined Professor William L. Hase's group at Texas Tech University, Lubbock, as a post-doctoral fellow, where he was involved in developing efficient integration schemes for direct dynamics simulations and applying chemical dynamics simulations to study different chemical reactions. His general research interests include electronic structure theory and chemical reaction dynamics.

**William L. Hase** is the Robert A. Welch Professor of Chemistry at Texas Tech University. He received his B.S. degree from the University of Missouri, Columbia (1967), and his Ph.D. from New Mexico State University (1970). He was a post-doctoral associate with Don Bunker, University of California, Irvine, before joining the faculty at Wayne State University (1973). He moved to Texas Tech University in 2004. Hase is a theoretical and computational chemist whose research interests include theories of chemical reaction dynamics and kinetics, algorithm and software development for chemical dynamics simulations, and applications of these simulations to a broad range of problems. He has a continual interest in the study of intramolecular and unimolecular dynamics. His research group has written and maintains the chemical dynamics computer program VENUS (cdssim.chem.ttu.edu), which is interfaced with electronic structure computer programs for performing direct dynamics simulations. Current interests of his research group include collisions of projectiles with surfaces, post-transition-state dynamics, interfacial heat transfer, and electronic nonadiabatic transitions (monte.chem.ttu.edu).

of vibrational adiabaticity is HOCO dissociation, for which it has been proposed[40] that the OH stretch is partially adiabatic.

Experiment and computation have been important players in the development of unimolecular rate theory, and the interplay between theory, experiments, and computation is illustrated in Figure 1. In addition to RRKM/QET, phase space theory (PST),[28,41,42] variational unimolecular theory,[43−46] and the statistical adiabatic channel model (SACM)[47] are also important approaches for interpreting unimolecular reaction rates. Experimental studies have been very important in the development of unimolecular rate theory. A set of classical thermal unimolecular dissociation studies versus temperature and pressure by Rabinovitch and co-workers,[36,48,49] and chemical activation experiments by Rabinovitch and others,[50−52] illustrated the broad applicability of RRKM/QET theory in interpreting experiments. Chemical activation experiments at high presssures[38,53] also provided information regarding the rate of vibrational energy flow within molecules. Experiments[54,55] for which molecules are vibrationally excited by overtone excitation of a local mode (e.g., the C−H or O−H bond) gave results in overall good agreement with RRKM theory.[56] Non-RRKM kinetics is observed for some reactions, particularly those with shallow potential energy wells and low barriers for unimolecular decomposition.[57,58]

A more detailed microscopic picture of a unimolecular reaction may be obtained from time domain experiments in which the number of reactant and/or product molecules is followed in real time.[59−65] Pronounced non-RRKM kinetics were observed for the $NO_2 \rightarrow NO + O$[63,64] and $CH_3CO \rightarrow CO + CH_3$[65] reactions.

At the most fundamental level, unimolecular dissociation occurs via resonance states, which may be viewed as an extension of the bound states into the vibrational/rotational continuum of the energized molecule.[2] The line width for a resonance state gives its lifetime and, therefore, its unimolecular rate constant. Thus, resolving all of the resonance states, in a specific energy range for an energized molecule, gives a detailed, fundamental understanding of the molecule's state-specific unimolecular kinetics. This type of experiment has been performed for $D_2CO$,[66] HFCO,[67] HCO,[68] DCO,[69] $CH_3O$,[70] HOCl,[71,72] $HN_3$,[73] and HONO[74] decomposition, and orders of magnitude fluctuations were observed for the resonance state rate constants in a small energy range.

Initiated by the unimolecular dynamics simulations of Bunker[75,76] for model triatomic molecules, computational chemistry had an enormous impact on the development of unimolecular rate theory. Properties of unimolecular reaction dynamics investigated and characterized by computational chemistry are listed in Table 1, and in the following sections, relationships between unimolecular reactants' Hamiltonians and their dissociation probabilities[11,26,57,75−95] and classical phase space structures[96−106] are discussed. Also considered are effects of nonrandom excitation,[11,17,77,79,82,83] classical−quantum correspondences,[98,102,107−114] state-specific unimolecular rate constants,[2,19,111,115−124] and non-IRC and non-RRKM post-transition-state dynamics.[57,90,125−139] Some of these calculations have been inductive and explanatory, in that potential energy functions have been used which do not represent a specific molecule or molecules but instead describe general properties of broad classes of molecules. Such calculations have provided the fundamental information needed for developing an accurate unimolecular rate theory. Other calculations have utilized accurate potential energy surfaces with a goal of attaining quantitative comparisons with experiment and obtaining atomic-level understandings of the experimental observations. In the following sections, important theoretical and computational contributions to our understanding of unimolecular reaction dynamics are described. The article concludes with some ideas concerning advances in computational studies and how they may assist in addressing unresolved issues in unimolecular reaction dynamics.

## II. Classical Dynamics of Unimolecular Decomposition

**A. RRKM Rate Constant and Intrinsic RRKM and Non-RRKM and Apparent Non-RRKM Behaviors.** The RRKM expression for the unimolecular rate constant $k(E,J)$ is derived

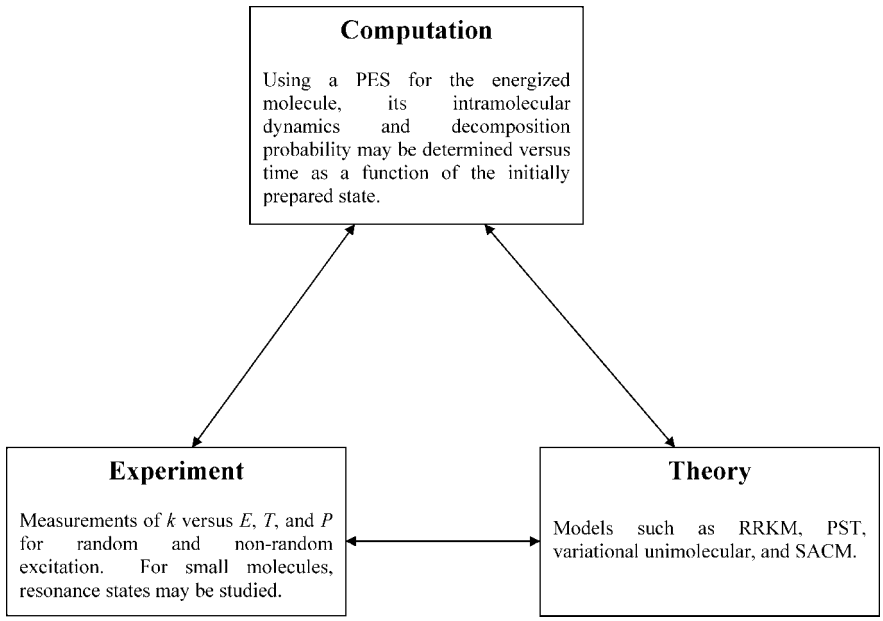


**Figure 1.** Interplay of theory, experiment, and computation for studies of unimolecular reaction dynamics.

**TABLE 1: Role of Computational Chemistry in the Development of Unimolecular Rate Theory**

| property of unimolecular dynamics | references |
|---|---|
| relationship between a unimolecular reactant's Hamiltonian (i.e., potential energy surface and atomic masses) and its dissociation probability (i.e., lifetime distribution); intrinsic RRKM and non-RRKM dynamics. | 11, 26, 57, 75−95 |
| effect of nonrandom excitation and an initial nonmicrocanonical ensemble of states; apparent non-RRKM dynamics | 11, 17, 77, 79, 82, 83 |
| relationships between unimolecular dynamics and classical phase space structures | 96−106 |
| classical−quantum correspondences | 98, 102, 107−114 |
| relationship between a unimolecular reaction's Hamiltonian and the exit channel potential energy release and product energy partitioning. | 10−13 |
| fluctuations in the state-specific unimolecular rate constants of resonances; mode-specific and statistical state-specific dynamics | 2, 19, 111, 115−124 |
| non-IRC and non-RRKM post-transition-state dynamics | 57, 90, 125−139 |

from classical mechanics.[12,18] A dividing surface, a classical mechanical construct, defines the transition state, which separates the energized reactant A* and product regions of phase space. If a microcanonical ensemble of states, that is, phase space points, is assumed for A* and if it is further assumed that trajectories crossing the dividing surface in the direct A* → products do not recross, the rate constant is an average of $\dot{q}_1\delta(q_1 - q_c)$, which is the average flux and magnitude of the unidirectional flow of phase space points through the dividing surface[140−142]

$$k(E,J) = \langle \dot{q}_1 \delta(q_1 - q_c) \rangle \tag{3}$$

Here, $q_1$ is the coordinate orthogonal to the dividing surface, that is, the reaction coordinate, and $q_c$ is the value of $q_1$ on the dividing surface.

Equation 3 may be rewritten in terms of phase space integrals for A* and the dividing surface (TS) and expressed as[12,18]

$$k(E,J) = \frac{\int\int \mathrm{d}p\mathrm{d}q\delta(H-E)\delta(q_1 - q_c)\dot{q}}{\int\int \mathrm{d}p\mathrm{d}q\delta(H-E)} \tag{4}$$

For a reactant with $s$ vibrational degrees of freedom, the numerator in eq 3 divided by $h^{s-1}$ is the TS's sum of states $N^{\ddagger}(E,J)$, and the denominator divided by $h^s$ is the reactant A*'s density of states $\rho(E,J)$, giving the traditional RRKM expression for $k(E,J)$, eq 1. The quantum RRKM expression for $k(E,J)$ is developed by replacing the classical $N^{\ddagger}(E,J)$ and $\rho(E,J)$ by their quantum counterparts.

The rapid IVR assumption of RRKM theory means that a microcanonical ensemble of A* states is maintained as A* decomposes so that, at any time $t$, $k(E,J)$ is given by

$$\frac{-\mathrm{d}N(t)}{\mathrm{d}t} = k(E,J)N(t) \tag{5}$$

As $k(E,J)$ does not depend on time, $N(t)$ decays exponentially, that is

$$N(t) = N(0)\exp[-k(E,J)t] \tag{6}$$

The lifetime distribution, $P(t)$,[76,140] is defined as

$$P(t) = -\frac{1}{N(0)}\frac{\mathrm{d}N(t)}{\mathrm{d}t} \tag{7}$$

and according to RRKM theory is given by

$$P(t) = k(E,J)\exp[-k(E,J)t] \tag{8}$$

Since a microcanonical ensemble is maintained at all times, a RRKM unimolecular system obeys the ergodic principle of statistical mechanics. Regardless of the form of $P(t)$, its intercept is the rate constant for the initial microcanonical ensemble, that is, $-\Delta N(t)/\Delta t = k(E,J)N(0)$, and is the RRKM constant.

In pioneering computations,[75,76] Bunker illustrated that chemical dynamics simulations may be used to determine the form of $P(t)$ for a molecule's decomposition. A unimolecular reactant whose lifetime distribution is in accord with eq 10 is identified as intrinsically RRKM.[77] $Al_6 \rightarrow Al_5 + Al$ dissociation behaves in this manner,[26] and its $P(t)$ is shown in Figure 2. A finding of Bunker, leading to extensive ensuing computations, is that not all molecular Hamiltonians have lifetime distributions in accord with eq 10. Model triatomic molecules with disparate force constants and/or masses, giving rise to a hierarchy of low and high vibrational frequencies have nonexponential $P(t)$ with an initial rate $-\mathrm{d}\ln P(t)/\mathrm{d}t$ larger than that of RRKM theory and a long-time rate constant much smaller than the RRKM $k(E,J)$.[75,76] A microcanonical ensemble of states is not main-

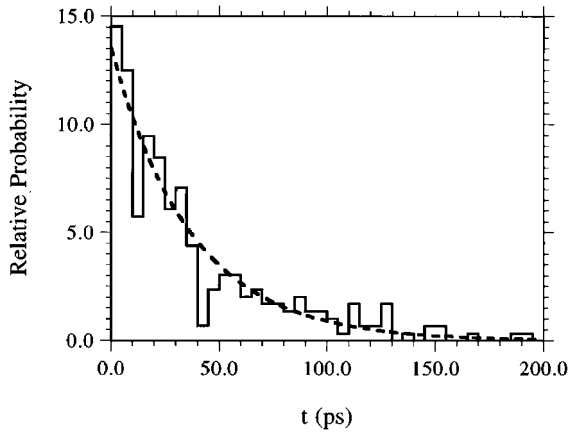


**Figure 2.** Trajectory $Al_6 \rightarrow Al_5 + Al$ lifetime distribution, following microcanonical sampling. The histogram plot represents the number of $Al_6$ dissociations per time interval. The dashed line represents the random lifetime distribution of eq 10. The energy is 40 kcal/mol, and the angular momentum is zero. Adapted from ref 26.

tained during the molecule's dissociation, and its unimolecular rate constant is time-dependent. Only at $t = 0$, when a microcanonical ensemble exists, does its rate constant equal the RRKM $k(E,J)$. Such unimolecular dynamics is identified as intrinsic non-RRKM.[77] Thus, for intrinsic non-RRKM behavior, a microcanonical ensemble is initially prepared, which uniformly covers the energized molecule's phase space. However, the unimolecular reaction "empties" certain domains of phase space faster than others, and intramolecular vibrational energy redistribution (IVR) cannot refill the depleted domains fast enough to maintain the microcanonical ensemble.

A nonexponential $P(t)$ for intrinsic non-RRKM dynamics may be expressed as

$$P(t) = \sum_i c_i e^{-k_i t} \tag{9}$$

Thus, from eq 7

$$N(t)/N(0) = \sum_i f_i e^{-k_i t} \tag{10}$$

and $c_i = f_i k_i$. In the absence of barrier recrossing, by definition, the sum of $c_i$ in eq 9 equals $k(E,J)$ since the initial decay is for a microcanonical ensemble. One of the $k_i$ in eq 9 may approximate the RRKM $k(E,J)$. An initial rate constant $-\mathrm{d}\ln P(t)/\mathrm{d}t$, larger than that of RRKM theory, suggests that the molecule is behaving smaller than its actual size. The possibility of such behavior was first proposed by Rice[143] of RRKM theory. A long-time rate, much smaller than the RRKM $k(E,J)$, suggests that decomposition of the long-time trajectories is not controlled by the transition state but by a "bottleneck" for transfer of energy into the coordinate(s) leading to decomposition.[76] Bunker's finding of non-RRKM dynamics was consistent with and followed earlier simulation by Fermi et al.[144] of nonrandom energy transfer in a linear chain. These unimolecular chemical dynamics simulations were pioneering in that they documented, by computational chemistry, that actual molecules may have non-RRKM unimolecular dynamics. The concept of intramolecular relaxation (i.e., IVR) and its role in ensuring RRKM dynamics was advanced.

Apparent non-RRKM behavior arises from nonrandom initial excitation, which forms an initial nonmicrocanonical ensemble with certain regions of phase space "filled-in" with higher probabilities than others.[77] An intrinsic RRKM molecule may be excited in this manner. As a result, the initial form of the lifetime distribution, including the intercept, may not be the exponential assumed by RRKM theory. Nevertheless, the RRKM assumption of rapid IVR requires the distribution of states to become microcanonical in a negligibly short time compared to the RRKM lifetime $1/k(E,J)$, resulting in a RRKM $P(t)$ following the initial non-RRKM short-time component. The extent of this component, and whether it enhances or suppresses initial reaction, depends on properties of the excitation process and where the energy is initially localized in the molecule. If the molecule is also intrinsically non-RRKM, its $P(t)$ will be a convolution of its apparent and intrinsic non-RRKM dynamics. The pioneering chemical activation experiments of Rabinovitch and co-workers[38,53] are classic examples of short-time apparent non-RRKM behavior and longer-time RRKM dynamics. A "well-behaved RRKM" molecule with fast IVR will not exhibit intrinsic non-RRKM dynamics and only apparent non-RRKM dynamics on a very short time scale.

**B. Phase Space Structures.** Trajectories for a microcanonical ensemble of states, selected for a unimolecular reactant, may have different types of motion.[2,103] The assumption of RRKM theory is that the internal motion of the energized molecule is irregular (i.e., chaotic), giving rise to ergodic dynamics on the time scale of the unimolecular reaction. Each of the molecule's phase space points has a random probability of reaching the TS dividing surface, and a microcanonical ensemble is maintained during its dissociation. However, as discussed above, this model is not correct for all unimolecular reactions, and it is of interest to consider properties of molecular Hamiltonians which give rise to nonergodic and intrinsic non-RRKM dynamics.

For very low energies, the molecule's energy is given by the separable normal-mode Hamiltonian

$$H = \sum_i H_i = \sum_i (P_i^2 + \lambda_i Q_i^2)/2 \tag{11}$$

for which the energy is a sum of the energies in the individual normal modes $(Q_i,P_i)$. Since each degree of freedom is uncoupled and moves independent of the other modes, the classical motion is regular, giving rise to quasiperiodic trajectories with no energy transfer between the modes. The trajectory moves in a restricted region of phase space which has the shape of an $n$-dimensional torus.[103] This Hamiltonian is only rigorously accurate for small displacements from equilibrium, and as energy is increased, anharmonic and vibration/rotation couplings, identified by $H'$, become increasingly important and must be added to the Hamiltonian.[12] However, numerical simulations[103,104] have shown that the presence of this perturbation is not sufficient for "destroying" the quasiperiodic motion and yielding ergodic dynamics. Vibrational degrees of freedom will not freely exchange energy as long as there are no resonance conditions for energy transfer, for example, $n_1\omega_1 - n_2\omega_2 \approx 0$ for a two-dimensional Hamiltonian. Such frequency matching known as "internal" or "anharmonic" resonances[104,106] begins to destroy some of the tori for the regular quasiperiodic motion as the energy is increased, and the fraction of the trajectories in the phase space with quasiperiodic motion, that is, $f_{qp}$, becomes smaller. At some energy, there are extensive overlapping resonances, and the number of regular trajectories becomes negligibly small, leading to ergodic dynamics. The role of these resonances is explained by the Kolmogorov−Arnold−Moser (KAM) theorem,[102] which states that if there are no resonances among a set of oscillators, the addition of a perturbation that is sufficiently small compared to the total energy does not make the system ergodic. Oxtoby and Rice[96] have shown that the

intrinsic non-RRKM dynamics that Bunker found for model triatomic Hamiltonians results from insufficient internal resonances to yield ergodic dynamics.

A simplistic phase space structure with intrinsic non-RRKM is one consisting of only regular and irregular trajectories, with the latter exhibiting chaotic intramolecular dynamics so that a microcanonical ensemble is maintained within the irregular region of phase space.[11] If a microcanonical ensemble is sampled at $t = 0$ for the molecule's phase space, the number of reactant molecules versus time is

$$N(t) = N_{qp}(0) + N_{ch}(0)\exp(-k_{ch}t) \quad (12)$$

where $k_{ch}$ is the rate constant for the irregular, chaotic region and the rate constant is zero for the regular, quasiperiodic region. Since the initial ensemble is microcanonical

$$\frac{-dN(t)}{dt} = k_{RRKM}N(0) = k_{ch}N_{ch(0)} \quad (13)$$

evaluated at $t = 0$. Thus, $k_{ch} = k_{RRKM}/f_{ch}$, where $f_{ch} = N_{ch}(0)/N(0)$ and is the chaotic fraction of phase space. The density of states for the irregular, chaotic trajectories is $f_{ch}\rho(E)$, where $\rho(E)$ is the total density. The unimolecular lifetime distribution is

$$P(t) = k_{RRKM}\exp(-k_{ch}t) \quad (14)$$

The intercept of $P(t)$ is still the RRKM $k(E,J)$, but the rate constant in the exponential is larger, reflecting the smaller volume of phase space in which the irregular trajectories move.

The above model does properly describe that, with nonergodic dynamics, the lifetime distribution for an initial microcanonical ensemble will have an initial component that decays faster than the RRKM rate. However, it does not explain the often quite complex nonexponential $P(t)$ found for intrinsic non-RRKM molecules. The complexity of the molecule's dynamics arises from the nonergodic structure of the molecule's multidimensional phase space. For a period of time, trajectories in the vicinity of regular trajectories retain some degree of regularity in their motion and are said to move on "vague tori".[100] Thus, they do not have the chaotic dynamics[103] assumed by RRKM theory. As a result, their lifetimes may be much longer than expected by RRKM theory. The chaotic regions of phase space, with irregular trajectories, are intermingled with the regions of phase space with regular and "somewhat" regular trajectories and are connected via an Arnold web[104,106] of anharmonic resonances. A classical microcanonical ensemble for an intrinsic non-RRKM molecule consists of chaotic, "vague tori", and quasiperiodic trajectories. Such a complex, nonergodic phase space structure leads to a nonexponential $P(t)$.

**C. Chemical Dynamics Simulations of Intrinsic and Apparent Non-RRKM Dynamics.** Extensive chemical dynamics simulations were performed to study intrinsic and apparent non-RRKM dynamics for H−C−C → H + C═C Hamiltonians,[80−83,120] which model H−C bond rupture for an alkyl radical to form an alkene. Different model PESs were studied, and most exhibited intrinsic non-RRKM dynamics. For the PES that most closely resembles that for the ethyl radical ($C_2H_5$), approximately 20% of the phase space, for the average thermal energy of dissociating molecules at 500−1000 K, consists of quasiperiodic trajectories.[81] Regular and irregular trajectories for this PES are depicted in Figure 3, where plots are given of the H−C versus C−C bond lengths, H−C bond length versus H−C−C angle, and C−C bond length versus H−C−C angle as a function of time. The trajectories are excited above the unimolecular threshold with the same total energy. The different motions for the trajectories are a reflection of where they are initiated in H−C−C's phase space. The regular trajectories are excited with a large fraction of the energy in the C−C bond. On the other hand, energy is more equally distributed between the H−C and C−C stretch and H−C−C bend degrees of freedom for the irregular trajectories. The regular trajectories exhibit quasiperiodic motion and are trapped in the H−C−C phase space for the $10^{-10}$ sec integration time of the classical trajectories. They may never dissociate and are classical analogues of resonance states exhibiting mode specificity.[111,114]

The above H−C−C → H + C═C PES has been used in a chemical dynamics simulation to study the unimolecular decomposition of H−C−C* formed by H + C═C association.[83] The number of the H−C−C* species surviving versus time, $N(t)$, is highly nonexponential, and a sum of three exponentials

$$N(t)/N(0) = \sum_{i=1}^{3} f_i \exp(-k_i t) \quad (15)$$

gives an excellent fit to the trajectory result. The fitted parameters are $f_1 = 0.689$, $f_2 = 0.248$, and $f_3 = 0.063$, $k_1 = 5.53 \times 10^{12}$ s$^{-1}$, $k_2 = 6.06 \times 10^{11}$ s$^{-1}$, and $k_3 = 1.1 \times 10^{11}$ s$^{-1}$. The short- and long-time rate constants, $k_1$ and $k_3$, differ by a factor of 50. The RRKM rate constant is $1.0 \times 10^{12}$ s$^{-1}$.

This $N(t)$ displays both apparent and intrinsic non-RRKM dynamics. At short lifetimes, the trajectory dissociation rate constant is larger than the RRKM value, consistent with the nonrandom nature of the excitation step, which preferentially samples regions of the H−C−C* phase space that are strongly coupled to the dissociation path. The rate constant for the long-time exponential tail of the trajectory $N(t)$ is an order of magnitude smaller than the RRKM value, and this has been attributed to trajectories moving on vague tori.[100] Regular quasiperiodic H−C−C* trajectories, present in the phase space,[81] cannot dissociate and are not coupled to the H + C═C products. Thus, they cannot be formed by H + C═C association. Though there are major differences between the trajectory and RRKM $N(t)$, within the statistical uncertainty, the trajectory average lifetime of $1.1 \times 10^{-12}$ s is identical to the microcanonical value of $1.0 \times 10^{-12}$ s, a rather surprising result discussed in the next section.

Trajectory calculations have also been used to study the unimolecular dynamics of ethyl radical dissociation,[11,84,85] that is, $C_2H_5 \rightarrow H + C_2H_4$, using an analytic PES fit to ab initio calculations.[145] In contrast to the above results for the model alkyl radical H−C−C, when $C_2H_5$ is excited with a microcanonical ensemble of states, it dissociates with an initial $P(t)$ consistent with RRKM theory and intrinsic RRKM dynamics. However, apparent non-RRKM behavior is present in a trajectory simulation of $C_2H_5$ nonrandomly excited by H + $C_2H_4$ association.[11] As shown in Figure 4, this leads to an initial dissociation rate that is faster than that of RRKM theory. This apparent non-RRKM component lasts for about 0.25 ps, and then, the rate constant (i.e., the slope of log $N$ versus $t$) attains the RRKM value of $7 \times 10^{10}$ s$^{-1}$.

More recent direct dynamics classical trajectory simulations of the intramolecular and unimolecular dynamics of $C_2H_5$ suggest that a fraction of the $C_2H_5$ phase space consists of vague tori and quasiperiodic trajectories.[146,147] For a 5 eV excitation energy, it is found that ~78% of a microcanonical ensemble of trajectories dissociates to H + $C_2H_4$ with a single exponential and a rate constant consistent with RRKM theory.[146] However, the remaining long-lived trajectories have motions consistent with vague tori and quasiperiodicity and a low degree of ergodicity.[147] These dynamics indicate that $C_2H_5$ dissociation is intrinsically non-RRKM. It is suggested[146] that these long-

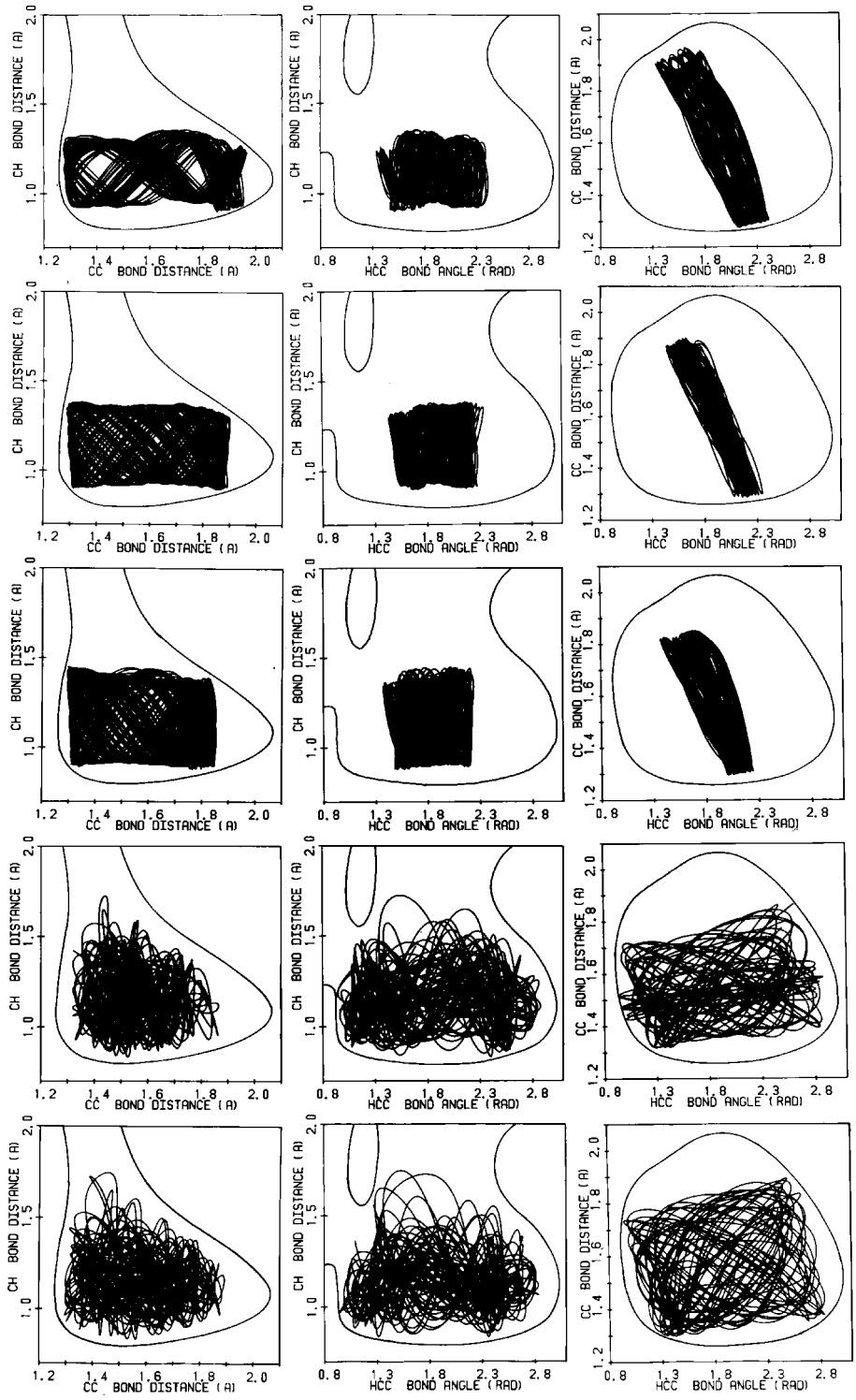


**Figure 3.** Regular and irregular trajectories for the model H−C−C → H + C═C reaction. Adapted from ref 81.

lived trajectories are prepared when $C_2H_5$ is photoexcited[148,149] and explain observed dissociation lifetimes which are several orders of magnitude longer than those expected from RRKM theory. These direct dynamics results are not inconsistent with the RRKM dynamics found in the above study using an analytic PES since it did not investigate long-lived trajectories.[84,85] It is also found[146] that the importance of vague tori and quasiperiodic trajectories in the $C_2H_5$ phase space depends strongly on the electronic structure method used for the direct dynamics, and some electronics structure theories may yield intrinsically non-RRKM dynamics. Though the thermal kinetics of $C_2H_5$ dissociation, including H, D isotopic substitution, appear to be well-described by RRKM theory,[150] as shown in the next section, thermal and collision-averaged rate constants are not particularly sensitive to intrinsic non-RRKM dynamics, and a that small fraction of the $C_2H_5$ phase space consists of vague tori and quasiperiodic trajectories may not be inconsistent with RRKM thermal kinetics.

**D. Non-RRKM Dynamics and Unimolecular Rate Constants Versus Energy, Temperature, and Pressure.** ***1. Rate Constant k(E).*** The phenomenological collision-averaged chemical activation rate constant is defined as[151]

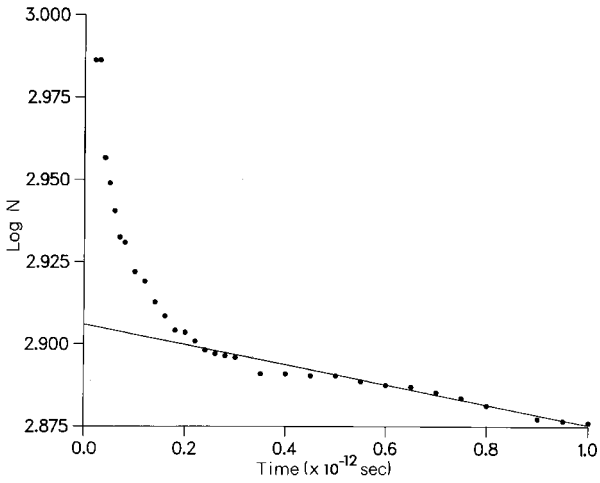


**Figure 4.** Classical trajectory lifetime distribution for decomposition of $C_2H_5$, formed by H + $C_2H_4$ association. Calculation of a H + $C_2H_4$ relative translational energy of 30 kcal/mol. Association deposits both this energy and the 40 kcal/mol reaction exothermicity nonrandomly into $C_2H_5$, preferentially exciting the formed C−H bond. Adapted from ref 11.

$$k(\omega, E) = \omega D/S \tag{16}$$

where $\omega$ is the collision frequency per molecule, $D$ is the probability of forming decomposition products, and $S$ is the probability of forming a collisionally stabilized reactant. A convenient way to represent $D$ and $S$ is to consider the lifetime distribution $P(t)$[140,152] in eq 7. In the simplest analysis, one assumes that collisions between bath molecules and the energized reactant are uncorrelated and that each collision results in stabilization. (One can modify the latter assumption for the case of "weak" collisions.[152−154]) The probability that the reactant avoids a collision for time $t$ is $W(t)$[140]

$$W(t) = \exp(-\omega t) \tag{17}$$

Since $P(t)\mathrm{d}t$ is the probability that a reactant molecule dissociates in the time interval $t \rightarrow t + \mathrm{d}t$, the total probability of dissociation is

$$D = \int_0^\infty W(t)P(t)\mathrm{d}t \tag{18}$$

The probability of stabilization $S$ equals $1 - D$, that is

$$S = 1 - \int_0^\infty W(t)P(t)\mathrm{d}t \tag{19}$$

Inserting the above expressions for $D$ and $S$ into eq 16 yields the unimolecular rate constant $k(\omega,E)$ as a function of $\omega$, that is, pressure.

Of particular interest are the low-pressure ($\omega \rightarrow 0$) and high-pressure ($\omega \rightarrow \infty$) limits of the unimolecular rate constants.[155] The expression for $k$ in the low-pressure limit is

$$k(0, E) = N(0)/\int_0^\infty N(t)\mathrm{d}t \tag{20}$$

For the high-pressure limit, one obtains

$$k(\infty, E) = P(0) \tag{21}$$

It is seen that $k(\infty,E)$ is equal to the lifetime distribution $P(t)$ evaluated in the limit $t \rightarrow 0$. In contrast, eq 20 does not provide direct information about $P(t)$ at $t \rightarrow \infty$ and the low-pressure limit. For intrinsic non-RRKM dynamics and the multiexponential $N(t)$ in eq 10

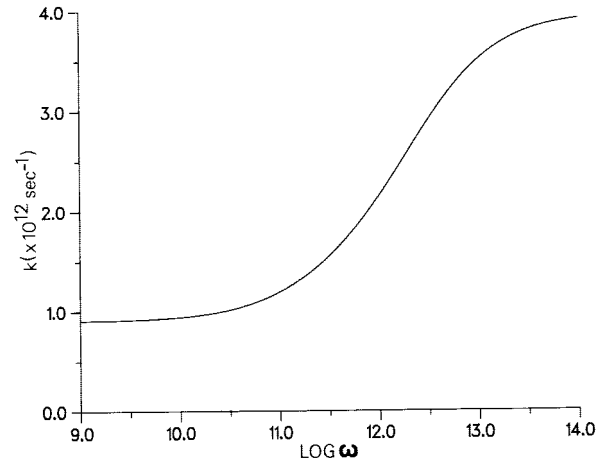


**Figure 5.** Plot of the chemical activation rate constant $k(\omega,E)$ versus $\omega$ (i.e., pressure) for excited model H−C−C* radicals formed by H + C═C association. The population of these radicals versus time is given by eq 15. Adapted from ref 83.

$$k(0, E) = (\sum_i f_i/k_i)^{-1} \tag{22}$$

A feature of eq 20 is that it does not require an exponential $N(E,t)$ for $k(0,E)$ to approximately equal the RRKM unimolecular rate constant $k_{RRKM}$. For the exponential decomposition of RRKM theory, eqs 6 and 7, $k(\omega,E)$ is independent of $\omega$, and both $k(\infty,E)$ and $k(0,E)$ equal $k_{RRKM}$.

A plot of $k(\omega,E)$ versus $\omega$ is given in Figure 5 for the dissociation of the model H−C−C* radicals described above,[83] whose population versus time is given by eq 15. The rate constant is pressure-dependent, as expected by the nonexponential $P(t)$. However, since $k(\omega,E)$ is a convolution of $W(t)$ and $P(t)$, the form of $P(t)$ is not apparent in the plot of $k(\omega,E)$ versus $\omega$. For example, there is no indication in the $k(\omega,E)$ versus $\omega$ plot of the extremely long-lived trajectories which make up the tail of the lifetime distribution. The limiting high- and low-pressure values of $k(\omega,E)$ are $k(\infty,E) = 3.97 \times 10^{12}$ $s^{-1}$ and $k(0,E) = 9.05 \times 10^{11}$ $s^{-1}$. The low-pressure rate constant is nearly identical to the RRKM rate constant of $1.0 \times 10^{12}$ $s^{-1}$.[80,82]

The significance of the finding that $k(0,E)$, for chemically activated H−C−C* dissociation, approximates $k_{RRKM}$ was investigated by considering a model in which the intramolecular phase space of the reacting molecule is treated as containing two or three regions, each with its own kinetic behavior, that is, two- and three-state models.[155] For the two-state model, the activation, intramolecular relaxation, and unimolecular dissociation are represented as

$$\text{initiation} \rightarrow N_1 \tag{23a}$$

$$N_1 \underset{k_3}{\overset{k_2}{\rightleftharpoons}} N_2 \tag{23b}$$

$$N_1 \xrightarrow{k_1} \text{products} \tag{23c}$$

where $k_2$ and $k_3$ are intramolecular energy-transfer rate constants. For the three-state model, the step

$$N_1 \underset{k_5}{\overset{k_4}{\rightleftharpoons}} N_3 \tag{24}$$

is added to the above scheme. With appropriate parameters, the three-state model provides an excellent fit to the trajectory $N(t)$.

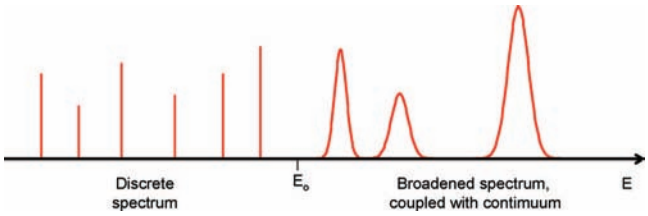


**Figure 6.** Possible absorption spectrum for a molecule which dissociates via isolated compound-state resonances. $E_o$ is the unimolecular threshold.

For the two- and three-state models, $k(\infty,E)$ equals $k_1$, as expected since this is the region of the phase space initially excited. For both models, an analytic expression for $k(0,E)$ is obtained and found to be identical to $k_{RRKM}$ for a microcanonical population of the $N_1$, $N_2$, and $N_3$ regions of phase space. This is a rather profound finding and is expected to exist for analogous $n$-state models. However, this has not been shown analytically.

***2. Rate Constant $k_{uni}(\omega,T)$.*** The monoenergetic unimolecular rate constant $k_{uni}(\omega,E)$ in the Lindemann−Hinshelwood mechanism for thermal unimolecular decomposition is related to the above $k(\omega,E)$ by[76,116,140,156]

$$k_{uni}(\omega,E)=\frac{\omega k(\omega,E)}{k(\omega,E)+\omega} \quad (25)$$

If the energy $E$ is assumed to be continuous,[156,157] one obtains $k_{uni}(\omega,T)$ by Boltzmann weighting the $k_{uni}(\omega,E)$ in eq 25; that is

$$k_{uni}(\omega,T)=\frac{\omega}{Q}\int_0^\infty \frac{k(\omega,E)\rho(E)\exp(-E/k_BT)}{k(\omega,E)+\omega}\mathrm{d}E \quad (26)$$

where $Q$ is the partition function for the reactant molecule's internal degrees of freedom. This expression is a further extension of the standard thermal Lindemann−Hinshelwood unimolecular rate constant[152−154] for it incorporates the standard RRKM model in which $k(\omega,E)$ equals the RRKM rate constant $k(E)$ as well as eqs 16−19 for a nonexponential lifetime distribution $P(t)$ and non-RRKM kinetics.

## III. Quantum Dynamics of Unimolecular Decomposition

**A. Resonance States: State-Specific Decomposition.**

***1. Mode Specificity.*** The above theoretical and computational models, including RRKM theory, describe unimolecular decomposition within the domain of classical mechanics. The quantum RRKM expression results from replacing the classical $N^\ddagger(E,J)$ and $\rho(E,J)$ by their quantum counterparts. Thus, it is of interest to consider the actual quantum dynamics of unimolecular decomposition. At the unimolecular threshold of moderate to large size molecules, there are many vibrational/rotational states within the experimental energy resolution d$E$, and accurate quantum calculations of unimolecular decomposition have not been performed for these molecules since there are uncertainties in defining the initial wave function $\Psi(0)$ and difficulties in propagating it for a moderate size molecule with a larger density of states. Instead quantum calculations have addressed small molecules and larger molecules at lower levels of excitation, which decompose via isolated compound-state (i.e., Feshbach) resonances. As shown in Figure 6, these resonances may be viewed as the extension of bound states into the dissociative continuum,[2] and since they are spectrally isolated, they have individual state-specific rate constants. The lifetime for the resonance is

$$\tau_n=1/k_n=\hbar/\Gamma_n \quad (27)$$

where $k_n$ is the resonance's unimolecular rate constant and $\Gamma_n$ the full-width at half-maximum of its Lorentzian-broadened absorption line shape. Thus, $k_n$, the primary variable, defines the resonance's lifetime.

There are extensive fluctuations in state-specific rate constants for resonances within a narrow energy interval.[66−74] However, this does not necessarily imply mode-specific unimolecular decomposition.[116b] What is required for mode-specific unimolecular decomposition is a distinguishable and, thus, assignable pattern (or patterns) in the positions of resonance states in the spectrum. Identifying such patterns in a spectrum allows one to determine which modes in the molecule are excited for the resonance state. It is, thus, possible to interpret particularly large or small state-specific rate constants in terms of mode-specific excitations. Therefore, mode specificity means that there are exceptionally large or small state-specific rate constants depending on which modes are excited and that the energies, for the resonance states yielding mode-specific behavior, can be predicted by finding patterns in the positions of these resonance states in the spectrum. Examples of mode-specific decomposition are found for the model H−C−C Hamiltonian,[111,114] HCO,[117,118] and HOCl,[122,124] for which resonance states with 0 or 1 quanta in the H−C stretch motion have particularly long lifetimes. Near the threshold $E_o$, the unimolecular resonance rate constants for HOCl vary by 7 orders of magnitude!

The ability to assign a group of resonance states, as required for mode-specific decomposition, implies that the complete Hamiltonian for these states is well-approximated by a zero-order Hamiltonian with eigenfunctions $\phi_i(m)$.[98] The $\phi_i$ are product functions of a zero-order orthogonal basis for the reactant molecule or, more precisely, product functions in a natural basis representation of the molecular states,[158] and the quantity $m$ represents the quantum numbers defining $\phi_i$. The wave functions $\psi_n$, for the compound-state resonances before they begin to leak toward products, are approximately given by

$$\psi_n=\sum_i c_{ni}\phi_i(m) \quad (28)$$

Resonance states in the spectra, which are assignable in terms of the zero-order basis, will have a predominant expansion coefficient $c_{ni}$. Hose and Taylor[98] have argued that for an assignable level, $c_{ni}^2 > 0.5$. Generally more than one zero-order Hamiltonian may be necessary to assign resonance states for different regions of the spectrum.

***2. Statistical State Specificity.*** In contrast to resonance states which may be assigned quantum numbers and exhibit mode-specific decomposition, there are states which are intrinsically unassignable. Because of extensive couplings, a zero-order Hamiltonian and its basis set cannot be found to represent wave functions $\psi_n$ for these states. The spectrum for these states is irregular without patterns, and fluctuations in the $k_n$ are related to the manner in which the $\psi_n$ are randomly distributed in coordinate space. If all of the resonance states which form a microcanonical ensemble have random $\psi_n$, and are thus intrinsically unassignable, a situation arises which is called statistical state-specific behavior.[116b]

Since the wave function coefficients of the $\psi_n$ are Gaussian random variables when projected onto $\phi_i$ basis functions for any zero-order representation,[159] the distribution of the state-specific rate constants $k_n$ will be as statistical as possible. If the $k_n$ within the energy interval $E \rightarrow E + \mathrm{d}E$ form a continuous

distribution, it is suggested[159,160] that the probability of a particular $k$ is given by the Porter−Thomas distribution[161,162]

$$P(k) = \frac{\nu}{2\bar{k}}\left(\frac{\nu k}{2\bar{k}}\right)^{((\nu-2)/2)} \frac{\exp(-\nu k/2\bar{k})}{\Gamma(1/2\nu)} \tag{29}$$

where $\bar{k}$ is the average state-specific unimolecular rate constant within the energy interval $E \rightarrow E + dE$

$$\bar{k} = \int_0^\infty kP(k)d(k) \tag{30}$$

and $\nu$ is the "effective number of decay channels". For $\nu > 2$, there is a maximum in $P(k)$ located at[156]

$$k_{max} = \frac{\nu - 2}{2}\bar{k} \tag{31}$$

Increasing the effective number of decay channels $\nu$ reduces the variance of the distribution $P(k)$, which for $\nu > 2$ may be studied by considering the second moment[116b]

$$\begin{aligned}\langle[(k - k_{max})/k_{max}]^2\rangle &= \int_0^\infty [(k - k_{max})/k_{max}]^2 P(k)dk \\ &= \frac{2(\nu + 1)}{(\nu - 2)^2}\end{aligned} \tag{32}$$

As $\nu$ becomes large, this moment approaches zero.

The connection between the Porter−Thomas $P(k)$ distribution and RRKM theory is made through the parameters $\bar{k}$ and $\nu$. The relationship between the average of the statistical state-specific rate constants $k$ and the RRKM rate constant has been studied analytically[115] by considering a separable Hamiltonian, whose decomposition path is semiclassical tunneling through a potential energy barrier. The average of the state-specific rate constants for a microcanonical ensemble, $\bar{k}$, is the same as that of the RRKM rate constant. However, this is not a general result and only pertains to state-specific decomposition by tunneling through a barrier, which defines the dividing surface needed to derive RRKM theory from classical (not quantum) mechanical principles. More general comparisons between the average state-specific rate constant $\bar{k}$ and the RRKM $k(E)$ have come from studies of the $H_2CO \rightarrow H_2 + CO$,[66,163] $HO_2 \rightarrow H + O_2$,[91,117] and $NO_2 \rightarrow O + NO$[63,64] dissociations, which are statistical state-specific. The $k_n$ for $HO_2$ dissociation are shown in Figure 7. For each of these three dissociations, the RRKM $k(E)$ and $\bar{k}$, the average of the $k_n$ for the small-energy interval $\Delta E$, are in good agreement. This is shown in Figure 7 for $HO_2$. Similarly, the fluctuations in the $k_n$ are well-represented by the Porter−Thomas distribution.

The parameter $\nu$ in eq 29 has also been related to RRKM theory. For decomposition by quantum mechanical tunneling, and tunneling probabilities much less than 1, one obtains[159,164]

$$\nu = \prod_{k=1}^{3N-7} \coth(\pi\omega_k^{\ddagger}/\omega_b) \tag{33}$$

where $\omega_k^{\ddagger}$ are the $3N - 7$ frequencies for the modes orthogonal to the tunneling coordinate and $\omega_b$ is the barrier frequency. The interesting aspect of eq 33 is that it shows $\nu$ to be energy-independent in the tunneling region. On the other hand, for energies significantly above the barrier[159,164]

$$\nu = N^{\ddagger}(E) \tag{34}$$

where $N^{\ddagger}(E)$ is the sum of states for the transition state. In this region, $\nu$ rapidly increases with an increase in energy, and the $P(k)$ distribution becomes more narrowly peaked.

A microcanonical ensemble of isolated resonances decays according to

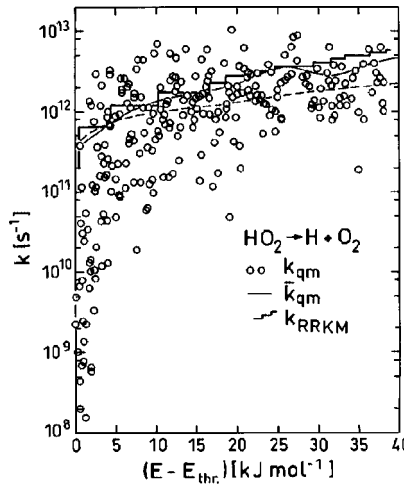


**Figure 7.** Comparison of the $HO_2 \rightarrow H + O_2$ unimolecular dissociation rates as obtained from quantum mechanical resonances ($k_{qm}$, open circles) and from variational transition-state RRKM theory ($k_{RRKM}$, step function). $E_{thr}$ is the threshold energy for dissociation. Also shown is the quantum mechanical average rate within an energy interval $\Delta E(\bar{k}_{qm}$, solid line) as well as the experimental prediction for $J = 0$ derived from a simplified SACM analysis of high-pressure unimolecular rate constants (dashed line). Adapted from ref 117 .

$$N(t, E) = \sum_n \exp(-k_n t) \tag{35}$$

which can be written as

$$N(t, E) = N_0 \int_0^\infty \exp(-k_n t)P(k)d(k) \tag{36}$$

if the state-specific rate constants are assumed continuous, with $N_0$ as the total number of molecules in the ensemble. For the Porter−Thomas $P(k)$ distribution, $N(t,E)$ becomes,[156,157]

$$N(t, E)/N_0 = (1 + 2\bar{k}t/\nu)^{-\nu/2} \tag{37}$$

In the limit $\nu \rightarrow \infty$, the right-hand side of eq 37 becomes the exponential $\exp(-\bar{k}t)$, as predicted by RRKM theory.

**B. State Specificity and Collision-Averaged Unimolecular Rate Constants.** Effects of nonexponential and non-RRKM unimolecular decomposition on the collision-averaged rate constants $k(\omega,E)$ and $k_{uni}(\omega,T)$ were discussed in section II.D. Here, we discuss how nonexponential decomposition, arising from state specificity, affects these rate constants. If the dissociation occurs via $N_0$ isolated resonance states in the energy interval $E \rightarrow E + \Delta E$, $k(\omega,E)$ is pressure-dependent and may be written as[116,156]

$$k(\omega, E) = N_0/\{\sum 1/(k_n + \omega)\} - \omega \tag{38}$$

with the high- and low-pressure limits of

$$k(\infty, E) = \langle k_n \rangle \tag{39}$$

$$k(0, E) = \langle 1/k_n \rangle^{-1} \tag{40}$$

Resonance states with small rate constants contribute more to $k(\omega,E)$ as the pressure is lowered, so that $k(\omega,E)$ decreases with a decrease in pressure. Equations 38−40 are for a specific application of eqs. 16, 21, and 22 and for the case that the nonexponential $N(t)$ in eq 15 is a sum of exponentials for the individual resonances.

Using eq 25, the monoenergetic unimolecular rate constant $k_{uni}(\omega,E)$ in the Lindemann−Hinshelwood mechanism for thermal unimolecular decomposition becomes[116b]

$$k_{\mathrm{uni}}(\omega, E) = \frac{\omega}{N_0}\sum_n \frac{k_n}{k_n + \omega} \quad (41)$$

where the summation is over the $N_0$ resonance states within $E \rightarrow E + \Delta E$. The high- and low-pressure limits of $k_{\mathrm{uni}}(\omega,E)$ are $\langle k_n \rangle$ and $\omega$, respectively. By summing over all of the resonance states, with the appropriate Boltzmann weighting, the following expression for the thermal Lindemann−Hinshelwood unimolecular rate constant is obtained

$$k_{\mathrm{uni}}(\omega, T) = \frac{\omega}{Q}\sum_n \frac{k_n \exp(-E_n/k_{\mathrm{B}}T)}{k_n + \omega} \quad (42)$$

For $\omega$ between the high- and low-pressure limits, state specificity makes the pressure-dependent rates significantly lower than the RRKM rates.[165a] This is observed in calculations of $k_{\mathrm{uni}}(\omega,T)$ for the state-specific decomposition of $HO_2$[165b] and HOCl.[165a] Hippler and co-workers[166] measured $k_{\mathrm{uni}}(\omega,T)$ for $HCO \rightarrow H + CO$ dissociation and found that only the isolated resonance model of eq 42, based on the quantum dynamics lifetimes, adequately described the observed $T$ and $P$ dependencies of the reaction rates.

If the dissociation of the resonance states is statistical state-specific and the distribution of resonance rates are that of Porter−Thomas and eq 29, simple expressions are obtained for $k(\omega,E)$ in the $\omega \rightarrow \infty$ and $\omega \rightarrow 0$ limits.[156] For the $\omega \rightarrow \infty$ limit, $k(\omega,E)$ is independent of $\nu$ and equals $\bar{k}$. At the $\omega \rightarrow 0$ limit, $k(\omega,E)$ depends upon the value of $\nu$. It equals 0 for a $\nu$ of 1 and 2 and equals $[(\nu - 2)/\nu]\bar{k}$ for $\nu > 2$ and finite. The latter value is the same as the value of $k$ for the maximum in $P(k)$ when $\nu > 2$ and finite, that is, eq 31. The state-specific rate constants of $H_2CO \rightarrow H_2 + CO$ dissociation are well-described by the Porter−Thomas distribution with $\nu = 4$.[66] For this case, $k(\omega,E)$ only decreases by a factor 2 in going from the high- to low-pressure limit. The pressure dependence of $k(\omega,E)$ becomes negligible as $\nu$ becomes very large. For the Porter−Thomas distribution, $P(k)$, $k_{\mathrm{uni}}(\omega,E)$ in eq 41 becomes

$$k_{\mathrm{uni}}(\omega, E) = \omega\int_0^\infty \frac{k}{k+\omega}P(k)\mathrm{d}k \quad (43)$$

Averaging over $E$ gives the Lindemann−Hinshelwood thermal unimolecular rate constant[116]

$$k_{\mathrm{uni}}(\omega, T) = \frac{1}{Q}\int_0^\infty \rho(E)k_{\mathrm{uni}}(\omega, E)\exp(-E/k_{\mathrm{B}}T)\mathrm{d}E \quad (44)$$

Equation 44 has been used to calculate $k_{\mathrm{uni}}(\omega,T)$ for the statistical state-specific dissociation of $HO_2$.[165b] Equation 44 is fundamentally the same as eqs 25 and 26. The rate constant $k_{\mathrm{uni}}(\omega,E)$ in eq 25 is defined for the nonexponential $N(t)$ in eq 15. In eq 44, $k_{\mathrm{uni}}(\omega,E)$ pertains to the nonexponential $N(t)$ in eq 35 for the microcanonical ensemble of resonance states. Bimolecular association reactions are related to unimolecular dissociations,[151] and the role of resonances in bimolecular associations has been treated theoretically.[167]

## IV. Accurate RRKM Rate Constants

**A. "Steps" in $k(E)$.** The quantity $N^{\ddagger}(E)$ in the quantum RRKM $k(E)$ expression increases incrementally as $E$ is increased. The minimum rate constant is at the threshold $E_o$ where $N^{\ddagger}(E_o) = 1$, that is, $k(E_o) = 1/h\rho(E)$. A stepwise increase is then predicted for $k(E)$ as additional states become available at the TS with an increase in $E$. The largest "step" is the first one for an increase in $N^{\ddagger}(E)$ from 1 to 2. As illustrated by the harmonic model for the TS's vibrational energy levels, the energy intervals, at which successive steps occur, are determined by the TS's vibrational frequencies, that is

$$E^{\ddagger}(\mathbf{n}^{\ddagger}) = \sum_{i=1}^{3N-7}(n_i^{\ddagger} + 1/2)h\nu_i^{\ddagger} \quad (45)$$

Thus, it would be possible to determine properties of the TS by experimental measurements of such steps, if they exist and are indeed described by quantum RRKM theory.

Though such steps have been suggested from experimental studies of ketene,[168] $NO_2$,[169] and acetaldehyde dissociation,[170] detailed analyses of the experiments suggest that the apparent steps in $k(E)$ do not arise from quantized transition-state energy levels.[171−173] Transition-state models used to interpret the steps are inconsistent with high-level ab intio calculations. These analyses have been reviewed by Grebenshchikov et al.[2] and summarized by Hase and Schinke,[19] who pointed out that the existence of steps is also inconsistent with the quantum dynamical calculations of unimolecular dissociation discussed in section III. As stated by Grebenshchikov et al., "In all quantum mechanical calculation which have been performed as well as in the few state-resolved experiments ($D_2CO$, $CH_3O$, HCO, and DCO) of unimolecular decomposition the resonance decay rates are found to fluctuate over several orders of magnitude. These fluctuations are especially pronounced and the distribution of rates is the widest near the dissociation threshold—exactly where the 'step' in the RRKM rate is expected to be the largest. The increase of the RRKM (i.e. average) rate by a factor of 2 is much smaller than the breadth of the distribution of rates—even if the narrowest resonances are not taken into account. Thus, the variation of the quantum mechanical rates in a small energy interval exceeds greatly the energy variation of $k(E)$ as predicted by RRKM theory at a 'step'. Moreover, an increase in $E$ so that $N^{\ddagger}(E)$ increases by 1 has little effect on the quantum distribution of the resonance rates—even at threshold." The latter is obvious in Figure 7, where the statistical state-specific resonance rate constants for $HO_2 \rightarrow H + O_2$ dissociation are depicted.

RRKM theory has its roots in classical mechanics, and the classical RRKM $k(E)$ is continuous without steps. Steps are introduced by the ad hoc introduction of the quantum $N^{\ddagger}(E)$, which is quantized. Grebenshchikov et al.[2] have also shown that "the existence of steps can be questioned by reviewing the main assumptions made in RRKM theory. First, the ad hoc replacement of the classical $N^{\ddagger}(E)$ by its quantum analogue neglects the state-specific nature of the coupling of the resonance states to the continuum. Second, the energy levels at the TS are defined in the adiabatic approximation, in which the 'slow' dissociation mode is decoupled from the 'fast' vibrational modes. In a more accurate description, non-adiabatic matrix elements, which couple the different adiabatic channels, have to be taken into account. They are usually not small at the TS where the potential 'perpendicular' to the reaction path and likewise the adiabatic vibrational wave functions change considerably as the reaction coordinate varies. Inclusion of non-adiabatic coupling would tend to smear out the 'steps'. Third, tunneling through the one-dimensional adiabatic potential energy curves also tends to round-off the step-like structures predicted by the RRKM expression as was convincingly demonstrated by model calculations for ketene by Gezelter and Miller."[172] RRKM theory requires ergodic dynamics for the reactant, with mixed unassignable states. If the TS has energy levels with well-defined quantum numbers, there is an extraordinary change in the dynamics in approaching the TS. Some special unimolecular reactions, which are highly vibrationally adiabatic, may have

steps. The importance of such vibrational adiabaticity has been discussed by Marcus.[174]

**B. The *K* Quantum Number: Adiabatic or Active.** There remains considerable uncertainty in how angular momentum should be treated in RRKM calculations.[39,175−181] Though the quantum number $J$ is a constant of the motion, the proper treatment of the $K$ quantum number, the projection of $J$ onto the molecular symmetry axis, is less certain. Coriolis coupling can mix the $2J + 1$ $K$ levels for a particular $J$ and destroy $K$ as a good quantum number. For this situation, $K$ is considered as an active degree of freedom. On the other hand, if the Coriolis coupling is weak, the $K$ quantum number may retain its integrity, and the unimolecular rate constant will depend on $K$ as well as $E$ and $J$. For this case, $K$ is an adiabatic degree of freedom.

It is straightforward to introduce active and adiabatic treatments of $K$ into the widely used RRKM model,[12] which represents vibrational and rotational degrees of freedom as harmonic oscillators and rigid rotors, respectively.[39,175] If $K$ is adiabatic, a molecule containing total vibrational−rotational energy $E$ and that is in a particular $J$, $K$ level has a vibrational density of states of $\rho[E - E_r(J,K)]$, where $E_r(J,K)$ is the rotational energy. Similarly, the transition state's sum of states for the same $E$, $J$, and $K$ is $N^{\ddagger}[E - E_o - E_r^{\ddagger}(J,K)]$, where $E_o$ is the unimolecular threshold. The RRKM rate constant for the $K$ adiabatic model is

$$k(E,J,K) = \frac{N^{\ddagger}[E - E_o - E_r^{\ddagger}(J,K)]}{h\rho[E - E_r(J,K)]} \tag{46}$$

For a microcanonical ensemble of states, the probability of $K$, $P(K)$, is proportional to the reactant molecule's vibrational density of states and is given by

$$P(K) = \frac{\rho[E - E_r(J,K)]}{\sum_{K=-J}^{J} \rho[E - E_r(J,K)]} \tag{47}$$

The microcanonical $k(E,J)$ for the $K$ adiabatic model is then

$$k(E,J) = \sum_{K=-J}^{J} P(K)k(E,J,K) \tag{48}$$

$$k(E,J) = \frac{\sum_{K=-J}^{J} N^{\ddagger}[E - E_o - E_r^{\ddagger}(J,K)]}{h\sum_{K=-J}^{J} \rho[E - E_r(J,K)]} \tag{49}$$

For the $K$ active model, mixing of the $2J + 1$ $K$ levels results in the following density and sum of states

$$\rho(E,J) = \sum_{K=-J}^{J} \rho[E - E_r(J,K)] \tag{50}$$

$$N^{\ddagger}(E,J) = \sum_{K=-J}^{J} N^{\ddagger}[E - E_o - E_r^{\ddagger}(J,K)] \tag{51}$$

The RRKM rate constant for the $K$ active model is obtained by inserting these expressions into eq 1 and is the same as $k(E,J)$ above for the $K$ adiabatic model. Thus, for a microcanonical ensemble of states, the $K$ adiabatic and $K$ active models give the same $k(E,J)$. However, the two models do give different rate constants for nonmicrocanonical ensembles of states or if the variational criterion is important for choosing the TS structure.[175] For these models, the treatment of $K$ is the same for the molecule and transition state. In addition, mixed mode models for $K$ may be formulated, in which $K$ is treated differently in the molecule and transition state,[39] to give a total of four models for treating the $K$ quantum number.

As expected, the sensitivity of $k(E,J,K)$ to $K$ tends to depend on the transition state's sum of states instead of the reactant's density of states since the rotational energy is a larger fraction of the transition state's total energy.[176] There are some $J,K$ levels for which $E_r^{\ddagger}(J,K)$ is greater than $E - E_o$, and thus, the unimolecular dissociation channel is closed. However, the $K$ dependence of $k(E,J,K)$ is also affected by the relationship between the reactant and TS moments of inertia, and it is expected that for many reactions, an interpretation of the $K$ dependence of $k(E,J,K)$ will require an understanding of how both $N^{\ddagger}(E,J,K)$ and $\rho(E,J,K)$ vary with $K$.

Differences in the above $K$ adiabatic and active models become apparent when considering the decomposition of an initial microcanonical ensemble of states $N(0)$.[175] For the $K$ active model, $N(t)$ will decay exponentially as $N(t) = N(0)\exp[-k(E,J,K)t]$. In contrast, for the $K$ adiabatic model, the decay is nonexponential and $N(t) = N(0)\sum_{K=-J}^{J} P(K)\exp(-k(E,J,K)t)$, with the $K$ states with the smallest rate constants preferentially remaining at long time. Detailed analyses of $N(t)$ for the $K$ adiabatic model indicate that striking nonexponential characteristics of $N(t)$ are only evident in its long-time tail, and evidence for a nonexponential $N(t)$ will be difficult to detect in experimental measurements of the collision-averaged rate constant $k(\omega,E)$ versus pressure, that is $\omega$.

If the variational criterion is important for choosing the TS, the $K$ adiabatic and active models will not give the same $k(E,J)$ and high-pressure-limiting rate constant $k_{uni}(\omega,T)$.[39,175] The $K$ adiabatic model will have a different TS structure for each $E$, $J$, $K$ ensemble and, thus, lower values for these rate constants. A similar relationship is found between PST rate constants calculated versus $E$, $J$, and $l$ ($l$ is the orbital angular momentum) and flexible variational RRKM rate constants versus $E$ and $J$ for an isotropic intermolecular potential between the product fragments.[182]

Whether the $K$ adiabatic or active model is used affects the calculation of the Lindemann−Hinshelwood thermal unimolecular rate constant $k_{uni}(\omega,T)$ in the $\omega \rightarrow \infty$ high-pressure limit, if the variational criterion is important (as discussed above).[39,165b] The treatment of $K$ also affects the shape of the falloff curve and is most pronounced at the $\omega \rightarrow 0$ low-pressure limit.[39,165b] At low pressure, $k_{uni}(\omega,T)$ is proportional to the effective collision frequency multiplied by the density of molecular states which can undergo unimolecular reaction. With $K$ adiabatic, there are molecular states for which $E_r^{\ddagger}(J,K)$ is greater than $E - E_o$, and there are no available states at the transition state through which reaction can occur. As a result, the $K$ adiabatic model has a smaller density of reactive molecular states, and it requires a larger effective collision frequency to fit experimental measurements of $k_{uni}(\omega,T)$ at low pressure. This effect is seen in calculations of $k_{uni}(\omega,T)$ for $C_2H_2Cl$[39] and $HO_2$[165b] dissociation. These calculations illustrate the interplay between parameters of RRKM models in fitting rate constants and point out that, until the proper model of $K$ is determined, it will not be possible to deduce physically meaningful collision efficiencies from thermal unimolecular rate constants.

**C. Anharmonicity.** A lingering and somewhat troubling issue in RRKM calculations is the inability to accurately represent anharmonic effects in calculating the TS's sum of states $N^{\ddagger}(E,J)$ and the reactant's density of states $\rho(E,J)$.[12,26,183] These anharmonic corrections are so often assumed to be negligible that the use of harmonic frequencies in calculating

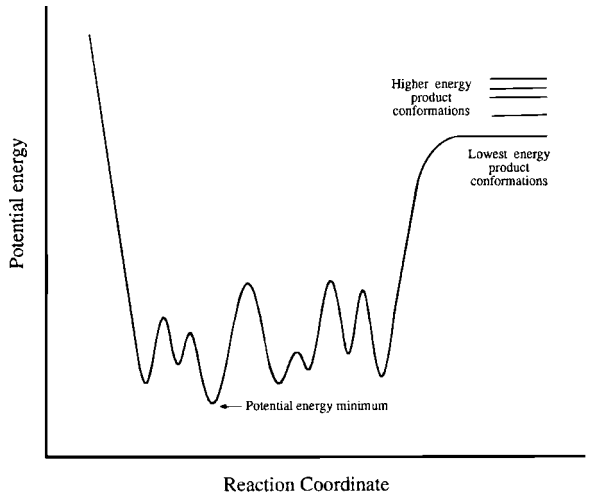


**Figure 8.** A model reaction coordinate potential energy curve for a fluxional molecule. Adapted from ref 26 .

$N^{\ddagger}(E,J)$ and $\rho(E,J)$ has, in many regards, incorrectly become known as RRKM theory. In reality, it is not clear that anharmonic corrections are negligible. If the anharmonic correct RRKM rate constant is $k_{anh}(E,J)$ and the harmonic approximation is $k_h(E,J)$, of interest is the size of $f_{anh}(E,J)$, that is[26,183]

$$k_{anh}(E,J) = f_{anh}(E,J)k_h(E,J) \quad (52)$$

For energies near and slightly above the unimolecular threshold, the anharmonic correction for $\rho(E,J)$ is expected to be significantly more important than that for $N^{\ddagger}(E,J)$, and a good approximation to $f_{anh}(E,J)$ is then $\rho_{anh}(E,J)/\rho_h(E,J)$. The ratio $\rho_{anh}(E)/\rho_h(E)$ has been measured for formaldehyde at 80 kcal/mol[66] and acetylene at 77 kcal/mol[184] and found to be 11 and 6, respectively. Quantum calculations for HCN at the H−C dissociation threshold of 124 kcal/mol give a factor of 8 for this ratio.[185] For the model molecule H−C−C, $\rho_{anh}(E)/\rho_h(E)$ determined from classical statistical mechanics is 2.95 at the dissociation energy of 90.0 kcal/mol.[186] There are two contributors to this factor, that is, 1.63 for the Morse stretch anharmonicity and 1.81 for bend−stretch coupling. For the three intermolecular modes of the $Cl^-\cdots CH_3Cl$ complex, $\rho_{anh}(E)/\rho_h(E)$ increases from 4 to 8 as the complex's excess energy is increased from 0.5 to 3.0 kcal/mol.[187] It is obvious that these corrections are not small, and attempts have been made to represent them by analytic functions to provide approximations for $f_{anh}(E,J)$.[183,188] Anharmonic corrections have also been approximated by representing each of a molecule's vibrational modes as a Morse oscillator.[189]

As illustrated in Figure 8, anharmonic corrections are expected to be very important for highly fluxional molecules, such as clusters and macromolecules, with multiple potential energy minima.[26] If these minima and their conformers are sampled randomly, within the time scale of the unimolecular reaction, they are all expected to contribute to the dissociating molecule's density of states. Classical statistical mechanics has been used to calculate anharmonic densities of states for the $Al_n$ clusters.[26] At energies equal to the $Al_6 \rightarrow Al_5 + Al$ and $Al_{13} \rightarrow Al_{12} + Al$ dissociation thresholds, the anharmonic density was found to be 56 and 4600 times larger than the harmonic density for $Al_6$ and $Al_{13}$, respectively. These calculations illustrate the critical importance of including anharmonic corrections to calculate accurate RRKM rate constants for fluxional molecules.

A classical mechanical value for $f_{anh}(E,J)$ may be obtained by comparing $k_{anh}(E,J)$ determined from a chemical dynamics simulations (i.e., the intercept of $P(t)$ for a microcanonical ensemble of initial states, as discussed in section II.A) with the approximate $k_h(E,J)$. This comparison gives $f_{anh}(E)$ values of 0.42[190] and 0.20[85] for $CH_4 \rightarrow H + CH_3$ and $C_2H_5 \rightarrow H + C_2H_4$ dissociation at 132 and 100 kcal/mol, respectively. Molozonide is formed by $O_3$ + propene association. A direct dynamics simulation of this process at 300 K, and the ensuing dissociation of molozonide, gives $f_{anh}(E) \sim 0.4$ for molozonide dissociation.[125] For large molecules with $s$ vibrational degrees of freedom and an energy $E$ substantially larger than the unimolecular threshold, the classical harmonic TST rate constant $k_h(T)$ is equivalent to the classical harmonic RRKM rate constant $k_h(E)$, where $E = \langle E \rangle = sk_BT \cong (s-1)k_BT$.[191] Thus, both of these rate constants have the same anharmonic correction factor, and one has

$$k_{anh}(E) = k_{anh}(T) = f_{anh}(E)k_h(E) = f_{anh}(T)k_h(T) \quad (53)$$

A value for $k_{anh}(E)$ may be determined from a chemical dynamics simulation, yielding $f_{anh}(E) = f_{anh}(T)$. It will be of considerable interest to determine the size of these anharmonic corrections and if they are indeed approximately unity for large molecules, as often assumed.[12]

## V. Illustrative Experimental Examples of Non-RRKM Dynamics

Above, non-RRKM dynamics for the decomposition of $C_2H_5$, HCO, HOCl, and the model alkyl radical H−C−C are described. In the next section, non-RRKM behavior associated with post-transition-state dynamics is discussed. Here, the non-RRKM dynamics observed experimentally for several molecules and reaction intermediates are presented to illustrate this behavior for different classes of chemical reactions and its prevalence in chemical kinetics. The importance of non-RRKM dynamics for thermal polyatomic reactions has been recently reviewed.[95]

**A. $X^- + CH_3Y$ $S_N2$ Nucleophilic Substitution.** The potential energy surface for $X^- + CH_3Y \rightarrow XCH_3 + Y^-$ $S_N2$ nucleophilic substitution has potential wells for the $X^-\cdots CH_3Y$ and $XCH_3\cdots Y^-$ ion−dipole complexes, which are separated by a $[X\cdots CH_3\cdots Y]^-$ central barrier.[29,30] Both chemical dynamics simulations[29,187,192] and experiments[193−196] show that the unimolecular kinetics of the prereaction $X^-\cdots CH_3Y$ complex is non-RRKM, which arises from weak coupling between the three $X^-\cdots CH_3Y$ intermolecular modes and the nine higher-frequency $CH_3Y$ intramolecular modes. The number of these complexes surviving versus time, following $X^- + CH_3Y$ association, is fit well by a multiexponential function as given eq 15.

For a trajectory simulation of $Cl^- + CH_3Cl$ association at 300 K,[192] $N(t)/N(0)$ for the $Cl^-\cdots CH_3Cl$ complex, eq 15, decays with $f_1 = 0.28$, $f_2 = 0.36$, and $f_3 = 0.36$, and $k_1 = 1.1$, $k_2 = 0.15$, and $k_3 = 0.093$ ps$^{-1}$.[187] The trajectory $N(t)/N(0)$ when averaged over collisions,[193] eqs 16−19, gives a $Cl^- + CH_3Cl \rightarrow Cl^-\cdots CH_3Cl$ association rate constant in very good agreement with the experimental value.[193,194] It is suggested that the long-time component in $N(t)$ arises from vague tori.[187]

The unimolecular dynamics of the $I^-\cdots CH_3I$ complex, formed by $I^- + CH_3I$ association, has been studied by time-resolved photoelectron spectroscopy.[195] The time dependence of the $I^-\cdots CH_3I$ complex is given by a biexponential curve, as in eq 15, with $f_1 = 0.78$, $f_2 = 0.22$, $k_1 = 1.5$ ps$^{-1}$, and $k_2 = 0.12$ ps$^{-1}$. The unimolecular dynamics of this $I^-\cdots CH_3I$ complex is very similar to that observed in the trajectory study, described above, of the $Cl^-\cdots CH_3Cl$ complex. Both complexes are formed by ion−molecule association.

Non-RRKM dynamics for $X^- \cdots CH_3Y$ complexes has been directly observed in experimental studies of $Cl^- \cdots CH_3Br$ ions.[196] When excited by a low-power CW $CO_2$ laser at 943 $cm^{-1}$, these ions only decompose to $ClCH_3 + Br^-$. In contrast, RRKM theory predicts that this excited $Cl^- \cdots CH_3Br$ complex should also decompose to $Cl^- + CH_3Br$. The mode of the complex excited by the 943 $cm^{-1}$ radiation is a $CH_3$ rocking intramolecular mode. That only the $ClCH_3 + Br^-$ products are observed is consistent with weak coupling between the complex's intramolecular and intermolecular modes since decomposition of $Cl^- + CH_3Br$ requires energy transfer from the initially excited $CH_3$ rock intramolecular mode to the $Cl^- \cdots C$ stretch intermolecular mode.

**B. Low-Barrier Isomerizations.** In experimental studies,[58,197−202] it has been discovered that thermal unimolecular rate constants for low-barrier isomerization reactions are often much smaller than the RRKM value and in some cases exhibit mode-specific effects. This work was initiated by Bauer and co-workers, and the isomerizations studied include those for aziridine,[197] chlorobutyne,[198] 2-fluoroethanol,[199] cyclohexanones,[200] flexible biomolecules,[201] nitrous acid,[202] and cyclopropane carboxaldehyde.[58] Low-barrier isomerization reactions appear to be a general class of reactions that are poorly described by RRKM theory.

A correction factor to the RRKM rate constant has been proposed for these isomerization reactions,[203−205] that is

$$k_{isom} = \kappa k_{RRKM} \qquad \kappa = \frac{k_{IVR}}{k_{IVR} + \nu_R} \tag{54}$$

where $k_{IVR}$ is the IVR rate and $\nu_R$ is the frequency of the motion of the reaction coordinate. The relationship of this $k_{isom}$ to the non-RRKM $P(t)$ is uncertain.

Following the discussion in section II, the unimolecular dynamics of these low-barrier isomerizations are intrinsically non-RRKM, with a bottleneck for energy flow into the reaction coordinate and reaching the TS. The observed unimolecular dynamics indicates that a microcanonical ensemble of states has a lifetime distribution $P(t)$ with an initial small component that has a rate constant much larger than that of RRKM theory and, then at longer times, a much larger single component or multiple components with a rate constant or constants much smaller than the RRKM value. In a collision environment, the pressure-dependent unimolecular rate constant is related to this non-RRKM $P(t)$ as described by eqs 16−19. For a microcanonical ensemble of reactant states, the collision-averaged rate constant $k(\omega,E)$ equals $k_{RRKM}$ at high pressure. If there is only a single longer time component in $P(t)$ following eq 22, $k(0,E) \approx k_2/f_2$, where $f_2 \gg f_1$ and $k_1 \gg k_2$. The rate constant $k_{isom}$ would then be associated with $k_2$ at low pressure. If the initial excitation is nonmicrocanonical (i.e., nonrandom), this will affect $P(t)$ and may also affect the observed rate constant. Time domain experiments of these isomerizations, in which the number of reactant and/or product molecules is followed in real time, would be very valuable.

It is of interest that non-RRKM dynamics has also been observed in both experiments[206] and simulations[207] for a unimolecular reaction involving a high-barrier isomerization. The acetone−enol cation $CH_3-COH-CH_2^+$ isomerizes to the acetone cation $CH_3-CO-CH_3^+$, which then dissociates to $CH_3^+$ and to $CH_3CO^+ + CH_3$. What is found is that the methyl group formed by this isomerization is $1.36 \pm 0.15$ times more likely to dissociate from the acetone cation, while RRKM theory predicts equal dissociation probabilities for the two $-CH_3$ groups.

**C. Collision- and Surface-Induced Dissociation.** In collision- and surface-induced dissociation (i.e., CID and SID), molecules are activated and then undergo unimolecular decomposition by collisions with projectiles and surfaces, respectively, and important non-RRKM dynamics has been observed in both experiments[24,208] and chemical dynamics simulations[23,209] for some of these processes. In $Ar + CH_3SH^+$ CID, the dominant product channel is $CH_3^+ + SH$,[208,209] even though it is 1.44 eV higher in energy than the lowest-energy channel yielding $CH_2SH^+ + H$. This has been explained by more efficient translational to vibrational energy transfer for the low-frequency C−S stretching mode than for the high-frequency C−H stretching modes and weak couplings between the low- and high-frequency vibrations giving rise to non-RRKM dyanamics and preferential C−S bond rupture.

Protonated peptide ions are activated by collisions with a surface in SID, and two different types of fragmentation mechanisms are observed.[23,24] For one, the traditional statistical mechanism, the ion rebounds off the surface and then fragments with the RRKM rate constant after undergoing efficient IVR. The second is a non-RRKM "shattering" mechanism,[23] in which the ion fragments as it collides with the surface. For these events, the ion is apparently properly oriented as it collides with the surface, so that the impact with the surface directly "drives" the ion to a fragmentation TS structure.

## VI. Direct Dynamics Simulations of Non-IRC and Non-RRKM Post-Transition-State Dynamics

RRKM theory is widely used to calculate lifetimes and branching ratios to different product channels for intermediates assumed to be trapped in "wells" on a PES. After passing a transition state, the intrinsic reaction coordinate (IRC)[210] for the minimum-energy path often leads to these wells. Furthermore, the PES may have additional wells that are not on the minimum-energy IRC but are accessible via IRCs with potential energy barriers smaller than those required to form products or return to reactants. A question of considerable interest is how accurately IRCs and RRKM theory identify the actual atomic-level mechanisms for chemical reactions. To contemplate the possible complexity of these post-transition-state dynamics,[125] consider standing at a high-energy rate-controlling transition state and gazing toward the reaction products and observing a "rough" multidimensional landscape, with multiple potential energy minima, reaction pathways, low energy barriers, and so forth connecting the transition state to multiple product channels. Given the range of possible dynamics resulting from the variety of these PES features, there is considerable interest in determining the actual post-transition-state dynamics for chemical reactions.

With increased computer speed and more powerful computer algorithms, it has become possible to perform direct dynamics simulations,[211] in which trajectories are integrated "on the fly" with the potential energy and its derivatives obtained directly from an electronic structure theory. This is a quite general computational methodology that has allowed the investigation of post-transition dynamics for numerous chemical reactions,[57,125−139] which are summarized in Table 2. The extensive non-IRC and non-RRKM dynamics observed in these simulations are striking. Also, in chemical dynamics simulations using analytic PESs, non-IRC dynamics, consistent with experiment, have been identified for $H_2CO$ and $CH_3CHO$ dissociation via the C−H bond rupture channel.[129−131] The dissociating H atom crosses a ridge on the PES and "falls" into the highly exothermic elimination dissociation channel, forming $H_2$ from $H_2CO$ and

**TABLE 2: Direct Dynamics Simulations of Gas-Phase Non-IRC and Non-RRKM Post-Transition-State Dynamics**

| chemical reaction and dynamics | electronic structure theory |
|---|---|
| thermal stereomutation of cyclopropane; trimethylene non-RRKM dynamics[57,132] | AM1-SRP |
| central barrier non-RRKM recrossing dynamics for the $Cl^- + CH_3Cl$ ($CD_3Cl$) $S_N2$ reaction[133] | MP2/6-31G* |
| non-RRKM dynamics of the biradical mediating vinylcyclopropane−cyclopentene rearrangement[134] | AM1-SRP |
| non-IRC cyclopropyl radical ring opening[135] | CASSCF(3,3)/6-31G* |
| $OH^- + CH_3F \rightarrow CH_3OH + F^-$ non-IRC and non-RRKM dynamics[136] | MP2/6-31+G* |
| Non-IRC and non-RRKM dynamics for 1, 2, 6-heptatriene rearrangement[127] | CASSCF(8,8)/6-31G* |
| heterolysis rearrangement of protonated pinacolyl alcohol[128] | HF/6-31G* |
| central barrier dynamics for the $Cl^- + C_2H_5Cl$ $S_N2$ reaction[137] | MP2/6-31G* |
| propene ozonolysis and molozonide non-RRKM unimolecular dissociation[125] | B3LYP/6-31G* |
| non-IRC and non-RRKM $E_{CO}2$ reaction mechanism for $F^- + CH_3OOH$[126] | B3LYP/6-311+G** |
| $O(^3P) + CH_3 \rightarrow H_2 + H + CO$ non-IRC dynamics[138] | B3LYP/6-31G* |
| $Cl^- + CH_3I \rightarrow ClCH_3 + I^-$ non-IRC and non-RRKM dynamics[139] | MP2/aug-cc-pVDZ |

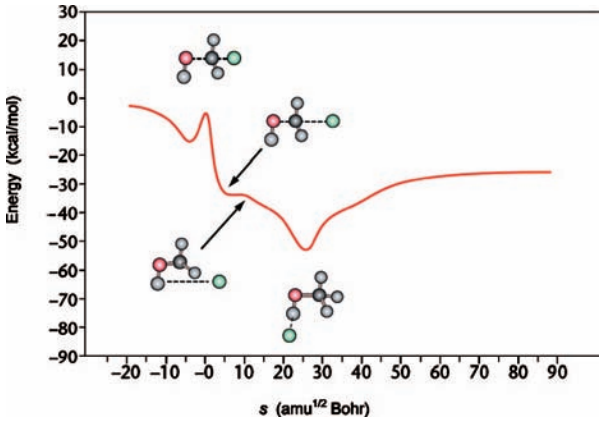


**Figure 9.** Potential energy along the intrinsic reaction coordinate (IRC) for $OH^- + CH_3F \rightarrow CH_3OH + F^-$; *s* is the distance along the reaction coordinate. This figure shows the structures at the potential energy minima and at the saddle point barrier. Adapted from ref 136.

$CH_4$ from $CH_3CHO$. Here, the non-IRC and non-RRKM dynamics found in chemical dynamics simulations of the $OH^- + CH_3F$[136] and $F^- + CH_3OOH$[126] reactions are reviewed. These are particularly interesting reactions since the non-IRC dynamical pathways avoid deep potential energy minima which are connected to the rate-controlling TS via the IRC.

**A. $[HO\cdots CH_3\cdots F]^- \rightarrow CH_3OH + F^-$.** The complete IRC for the $OH^- + CH_3F \rightarrow CH_3OH + F^-$ reaction, connecting the central barrier to the reactant and product asymptotic limits, was calculated at the MP2/6-31+G* level of theory. Energies and geometries along the IRC are shown in Figure 9. The IRC/RRKM mechanism is an indirect process with the system temporarily trapped in the $CH_3OH\cdots F^-$ minimum.

The direct dynamics trajectories were initiated at the central barrier TS,[136] with conditions chosen from a 300 K Boltzmann distribution for each of the TS's degrees of freedom, including reaction coordinate translation. The trajectories have two reaction pathways, one direct and the other indirect, and neither is the pathway predicted by the IRC in Figure 9. The vast majority, ~90%, follow a direct reaction pathway with departure of the $F^-$ ion approximately along the $O-C\cdots F^-$ collinear axis. The remaining small fraction of trajectories initially follows the direct pathway, but they do not have sufficient $CH_3OH + F^-$ relative translational energy to dissociate and are drawn into the $CH_3OH\cdots F^-$ minimum and form the IRC/RRKM intermediate. The origin of the preference for the direct reaction path is seen in Figure 10, in which the potential energy is plotted versus the $C\cdots F^-$ distance and $O-C\cdots F^-$ angle. As the system moves off the central barrier, it is propelled toward the products, avoiding the potential energy well and not forming the $CH_3OH\cdots F^-$ intermediate.

**B. $F^- + CH_3OOH$.** In recent experiments, Kato and coworkers studied the 300 K kinetics of the base-mediated decomposition reaction $F^- + CH_3OOH$.[212] Much to their surprise, the reaction did not yield the most exothermic products $HF + CH_2(OH)O^-$ and products predicted by the IRC. Instead, they proposed that the much higher energy non-IRC products $HF + CH_2O + OH^-$ were formed. The potential energy diagram of the $F^- + CH_3OOH$ reaction, calculated at the B3LYP/6-311+G** level of theory[126] is shown in Figure 11.

To provide an atomic-level understanding of the non-IRC dynamics observed in the experiments, a direct dynamics simulation was performed of the $F^- + CH_3OOH$ reaction.[131] To study the dynamics for the two pathways in which $F^-$ attacks the H atoms of the OH and $CH_3$ groups, trajectories were initiated for the $F^- + CH_3OOH$ reactants with initial conditions to model the 300 K experiments. The trajectories were integrated for 4 ps. It was found that 22.5% formed $HF + CH_2O + OH^-$, the major product reaction channel observed in the experiment,[212] 48.5% became trapped in the $CH_3OOH\cdots F^-$ potential energy well and formed a reaction intermediate that lasted up to the 4 ps of the trajectory integration, 1.5% formed the $HF + CH_3OO^-$ reaction products, and the remaining 27.5% went back to the reactants. None of the trajectories formed the IRC complex. The long lifetime for $CH_3OOH\cdots F^-$ is consistent with RRKM theory. That none of the trajectories followed the IRC is consistent with the experimental study.[212] The trajectory total reaction rate constant for $F^- + CH_3OOH$ is $(1.70 \pm 0.7) \times 10^{-9}$ cm$^3$/molecule·s and in excellent agreement with the experimental value of $1.23 \times 10^{-9}$ cm$^3$/molecule·s.

If the $CH_3OOH\cdots F^-$ complexes remaining, when the trajectories are terminated at 4 ps, are assumed to dissociate as predicted by RRKM, nearly all will form the $HF + CH_2O + OH^-$ products since the barrier is 16.4 kcal/mol lower for this channel as compared to the $HF + CH_3OO^-$ channel. With this assumption, the branching between the $HF + CH_2O + OH^-$ and $HF + CH_3OO^-$ product channels is predicted to be $0.98 \pm 0.01$ and $0.02 \pm 0.01$, fractions in qualitative agreement with the experimental results. The experimental estimates are ap-

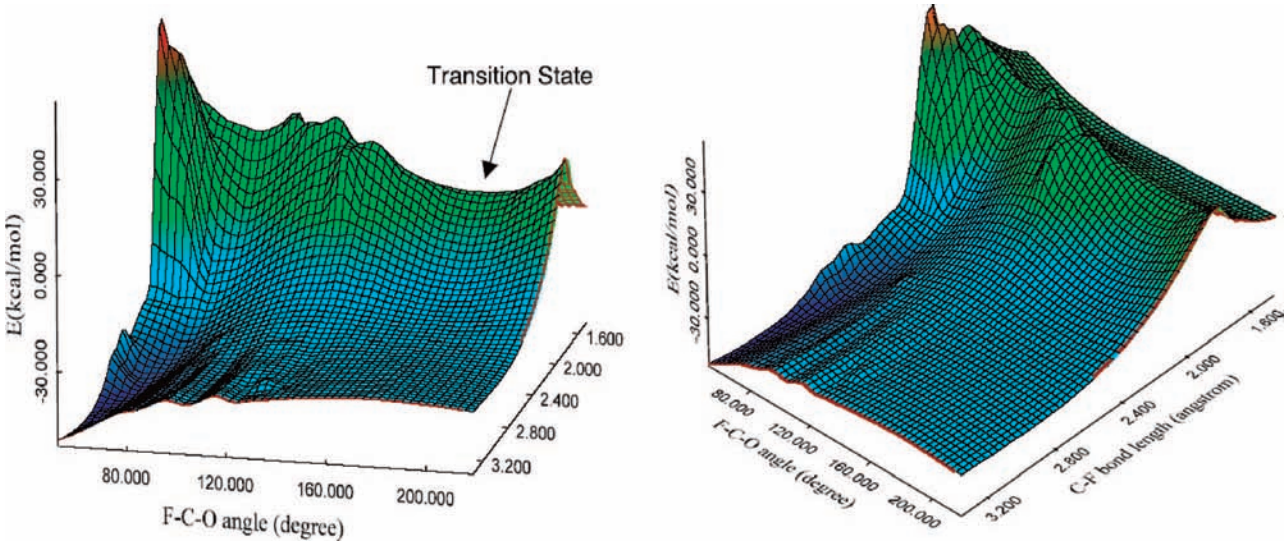


**Figure 10.** Potential energy contour diagram for $[HO\cdots CH_3\cdots F]^-$ fragmentation as a function of C−F distance and the O−C···F angle. The remaining coordinates are optimized at each point on the PES. Adapted from ref 136.

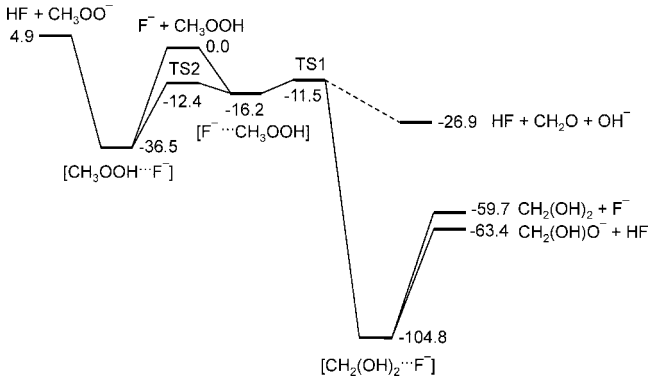


**Figure 11.** Energy diagram for the $F^- + CH_3OOH$ reaction at the B3LYP/6-311+G** level of theory. The energies shown are in kcal/mol and are relative to the $F^- + CH_3OOH$ reactant channel. Zero-point energies are not included. Adapted from ref 126.

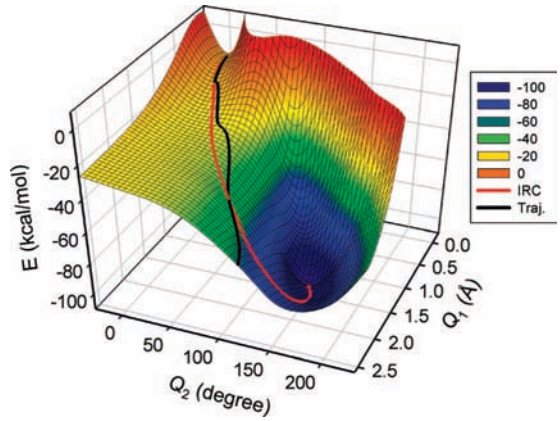


**Figure 12.** A two-dimensional contour diagram of the post-transition-state potential energy surface for $F^-$ attack of the $CH_3$ group of $CH_3OOH$. $Q_1 = \Delta r_1 + \Delta r_2$, where $r_1$ is the FH−C bond length and $r_2$ is the O−OH bond length. $Q_2 = \Delta\theta_1 + \Delta\theta_2$, where $\theta_1$ is the O−C−O angle and $\theta_2$ is the H−O−C angle, that is, H is the hydrogen abstracted by $F^-$ and O is the oxygen attached to carbon. $Q_1$ represents the concerted motion of HF and $OH^-$ away from $CH_2O$, and $Q_2$ represents rotation of $CH_2O$. The remaining coordinates were optimized for each $Q_1$, $Q_2$ point. Depicted on this contour diagram is the IRC (red line) and a representative trajectory (black line). Adapted from ref 126.

proximately 85 and 10% for these two channels. The trajectory estimate of only ~2% branching to the $HF + CH_3OO^-$ products is not inconsistent with the experiments, based on a difficult numerical analysis.[212]

A two-dimensional contour diagram of the post-transition-state potential energy surface for $F^-$ attack of the $CH_3$ group is illustrated in Figure 12. $Q_1$ represents the concerted movement of HF and $OH^-$ away from $CH_2O$, and $Q_2$ represents the inplane rotation motion of $CH_2O$. Also depicted in Figure 12 is the IRC and the motion for a representative trajectory. The trajectory "skirts" the deep potential energy minimum of the $CH_2(OH)_2\cdots F^-$ IRC complex and has non-IRC dynamics reminiscent of those above for the $OH^- + CH_3F \rightarrow CH_3OH + F^-$ reaction.

**C. Non-IRC Post-Transition Dynamics, Time Scales, and IVR.** The above simulations illustrate that the evaluation of PES features such as well depths, barrier heights, and intrinsic reaction coordinates may be insufficient for determining atomic-level mechanisms for chemical reactions. Instead, it is often necessary to study the actual motion of the atoms on a reactive system's PES. The efficiency of the reactive system to follow the IRC and form reaction intermediates in deep potential energy minima is intimately linked to the hierarchy of time scales for intramolecular motions and structural transitions on the PES and closely related to the concept of intramolecular vibrational energy redistribution (IVR).[14,15] To remain on the multidimensional IRC, the reaction coordinate translational energy acquired by the post-TS potential energy release must be transferred to the remaining degrees of freedom. This may become more efficient as the size of the reactive system increases, but there is no certainty that this is the case. For the $OH^- + CH_3F$ reaction, there is very weak coupling between $CH_3OH + F^-$ relative translation and $O-C\cdots F^-$ bending and other vibrational degrees of freedom, and the reactive system leaves the IRC. For the $F^- + CH_3OOH$ reaction, it is the weak coupling between the HF and $OH^-$ translations, $CH_2O$ rotation, and other motions which lead to the non-IRC dynamics.

## VII. Concluding Remarks

Computational studies have provided extensive information concerning the actual atomic level dynamics of unimolecular reactions, for example, RRKM and non-RRKM behavior, and broader applications of such work is expected. The quantum

dynamical calculations may be extended to larger molecules, providing more information regarding state-specific unimolecular decomposition. An atomic-level understanding of the origin of the extensive non-RRKM dynamics observed for some classes of reactions, for example, $S_N2$ nucleophilic substitution and low-barrier isomerizations, is needed. Extensive applications of direct dynamics simulations to many molecules and classes of molecules will provide a wealth of information concerning unimolecular dynamics and will be critical to understanding and interpreting experimental studies. These studies will provide challenges to the development of theoretical models for unimolecular reactions that can explain the observed nonstatistical dynamics.

**Acknowledgment.** The study of unimolecular reaction dynamics by the Hase research group, monte.chem.ttu.edu, has been primarily supported by the National Science Foundation, with additional support from the Air Force Office of Scientific Research, Office of Naval Research, and the Robert A. Welch Foundation. Bill Hase wishes to give special acknowledgements to his important collaborations concerning unimolecular dynamics with Reinhard Schinke, Tom Baer, and Kihyung Song and acknowledge additional collaborations with Rudy Marcus, Bruce Garrett, Bill McCurdy, Bob Gilbert, Bill Kaiser, Berny Schlegel, Mike Page, Don Setser, Chuck Doubleday, Evelyn Goldfield, Al Viggiano, Emilio Martínez-Núñez, Saulo Vásquez, and Theresa Windus.

## References and Notes

(1) Steinfeld, J. I.; Francisco, J. S.; Hase, W. L. *Chemical Kinetics and Dynamics*, 2nd Ed.; Prentice-Hall: Upper Saddle River, NJ, 1998; p 326.

(2) Grebenshchikov, S. Yu.; Schinke, R.; Hase, W. L. In *Comprehensive Chemical Kinetics, Vol. 39, Unimolecular Kinetics Part 1. The Reaction Step*; Green, N. J. B., Ed.; Elsevier: New York, 2003; p 105.

(3) Chan, S. C.; Rabinovitch, B. S.; Bryant, J. T.; Spicer, L. D.; Fujimoto, T.; Lin, Y. N.; Pavlou, S. P. *J. Phys. Chem.* **1970**, *74*, 3160.

(4) Troe, J. *J. Chem. Phys.* **1977**, *66*, 4745.

(5) Oref, I.; Tardy, D. C. *Chem. Rev.* **1990**, *90*, 1407.

(6) Flynn, G. W.; Parmenter, C. S.; Wodtke, A. M. *J. Phys. Chem.* **1996**, *100*, 12817.

(7) Liu, C.-L.; Hsu, H.-C.; Lyu, J.-J.; Ni, C.-K. *J. Chem. Phys.* **2006**, *124*, 054302.

(8) Havey, D. K.; Liu, Q.; Li, Z.; Elioff, M.; Fang, M.; Neudel, J.; Mullin, A. S. *J. Phys. Chem.* **2007**, *111*, 2458.

(9) Marcus, R. A. *J. Chem. Phys.* **1975**, *62*, 1372.

(10) Hase, W. L.; Bhalla, K. C. *J. Chem. Phys.* **1981**, *75*, 2807.

(11) Hase, W. L.; Buckowski, D. G.; Swamy, K. N. *J. Phys. Chem.* **1983**, *87*, 2754.

(12) Baer, T.; Hase, W. L. *Unimolecular Reaction Dynamics. Theory and Experiments*; Oxford: New York, 1996.

(13) Sun, L.; Park, K.; Song, K.; Setser, D. W.; Hase, W. L. *J. Chem. Phys.* **2006**, *124*, 064313.

(14) Hase, W. L. *J. Phys. Chem.* **1986**, *90*, 365.

(15) Uzer, T.; Miller, W. H. *Phys. Rep.* **1991**, *199*, 73.

(16) Nesbitt, D. J.; Field, R. W. *J. Phys. Chem.* **1996**, *100*, 12735.

(17) Hase, W. L. In *Modern Theoretical Chemistry, Vol. 2, Dynamics of Molecular Collisions, Part B*; Miller, W. H., Ed.; Plenum: New York, 1976.

(18) Hase, W. L. In *Encyclopedia of Chemical Physics and Physical Chemistry*; Moore, J. H. and Spencer, N. D., Eds.; Institute of Physics: Philadelphia, 2001; Vol. I, p 865.

(19) Hase, W. L.; Schinke, R. In *Theory and Applications of Computational Chemistry: The First Forty Years*; Dykstra, C., Frenking, G., Kim, K. S., Scuseria, G. E., Eds.; Elsevier: New York, 2005; p 397.

(20) Barker, J. R.; Golden, D. M. *Chem. Rev.* **2003**, *103*, 4577.

(21) Pilling, M. J.; Robertson, S. H. *Annu. Rev. Phys. Chem.* **2003**, *54*, 245.

(22) Maranzana, A.; Barker, J. R.; Tonachini, G. *Phys. Chem. Chem. Phys.* **2007**, *9*, 4129.

(23) (a) Meroueh, O.; Wang, Y.; Hase, W. L. *J. Phys. Chem. A* **2002**, *106*, 9983. (b) Wang, Y.; Hase, W. L.; Song, K. *J. Am. Chem. Soc. Mass Spectrom.* **2003**, *14*, 1402.

(24) Laskin, J.; Futrell, J. H. *J. Am. Soc. Mass Spectrom.* **2003**, *14*, 1340.

(25) Park, K.; Song, K.; Hase, W. L. *Int. J. Mass Spectrom.* **2007**, *265*, 326.

(26) Peslherbe, G. H.; Hase, W. L. *J. Chem. Phys.* **1996**, *105*, 7432.

(27) Peslherbe, G. H.; Hase, W. L. *J. Phys. Chem. A* **2000**, *104*, 10556.

(28) Chesnavich, W. J.; Bowers, M. T. In *Gas Phase Ion Chemistry*; Bowers, M. T., Ed.; Academic Press: New York, 1979; Vol. 1, p 119.

(29) Hase, W. L. *Science* **1994**, *266*, 998.

(30) Chabinyc, M. L.; Craig, S. L.; Regan, C. K.; Brauman, J. I. *Science* **1998**, *279*, 1882.

(31) Marcus, R. A.; Rice, O. K. *J. Phys. Colliod Chem.* **1951**, *55*, 894.

(32) Marcus, R. A. *J. Chem. Phys.* **1952**, *20*, 359.

(33) Rosenstock, H. M.; Wallenstein, M. B.; Wahrhafting, A. L.; Eyring, H. *Proc. Natl. Acad. Sci. U.S.A.* **1952**, *38*, 667.

(34) Bohr, N.; Wheeler, J. A. *Phys. Rev.* **1939**, *56*, 426.

(35) Mott, N. F.; Massey, H. S. W. *The Theory of Atomic Collisions*; Oxford: London, 1949; p 176.

(36) Schneider, F. W.; Rabinovitch, B. S. *J. Am. Chem. Soc.* **1962**, *84*, 4215.

(37) Whitten, G. Z.; Rabinovitch, B. S. *J. Chem. Phys.* **1964**, *41*, 1883.

(38) Rynbrandt, J. D.; Rabinovitch, B. S. *J. Phys. Chem.* **1971**, *75*, 2164.

(39) Zhu, L.; Hase, W. L.; Kaiser, E. W. *J. Phys. Chem.* **1993**, *97*, 311.

(40) Chen, W.-C.; Marcus, R. A. *J. Chem. Phys.* **2005**, *123*, 094307.

(41) Light, J. C. *Discuss. Faraday Soc.* **1967**, *44*, 14.

(42) Klots, C. E.; Mintz, D.; Baer, T. *J. Chem. Phys.* **1977**, *66*, 5100.

(43) (a) Hase, W. L. *J. Chem. Phys.* **1972**, *57*, 730. (b) Hase, W. L. *Acc. Chem. Res.* **1983**, *16*, 258.

(44) Chesnavich, W. J.; Bass, L.; Su, T.; Bowers, M. T. *J. Chem. Phys.* **1981**, *74*, 2228.

(45) Wardlaw, D. M.; Marcus, R. A. *Adv. Chem. Phys.* **1987**, *70*, 231.

(46) Klippenstein, S. J. *J. Phys. Chem.* **1994**, *98*, 11459.

(47) Quack, M.; Troe, J. *Ber. Bunsen-Ges. Phys. Chem.* **1974**, *78*, 240.

(48) Schneider, F. W.; Rabinovitch, B. S. *J. Am. Chem. Soc.* **1963**, *85*, 2365.

(49) Maloney, K. M.; Pavlou, S. P.; Rabinovitch, B. S. *J. Phys. Chem.* **1969**, *73*, 2756.

(50) Setser, D. W.; Rabinovitch, B. S. *Can. J. Chem.* **1962**, *40*, 1425.

(51) Johnson, R. L; Setser, D. W. *J. Phys. Chem.* **1967**, *71*, 4366.

(52) Hase, W. L.; Simons, J. W. *J. Chem. Phys.* **1970**, *52*, 4004.

(53) Meagher, J. F.; Chao, K. J.; Barker, J. R.; Rabinovitch, B. S. *J. Phys. Chem.* **1971**, *78*, 2535.

(54) Jasinski, J. M; Frisoli, J. K.; Moore, C. B. *J. Chem. Phys.* **1983**, *79*, 1312.

(55) Crim, F. *Annu. Rev. Phys. Chem.* **1984**, *35*, 657.

(56) Hase, W. L. *Chem. Phys. Lett.* **1985**, *116*, 312.

(57) Doubleday, C., Jr.; Bolton, K.; Hase, W. L. *J. Am. Chem. Soc.* **1997**, *119*, 5251. (b) Doubleday, C., Jr.; Bolton, K.; Hase, W. L. *J. Phys. Chem. A* **1998**, *102*, 3648.

(58) Dian, B. C.; Brown, G. G.; Douglass, K. O.; Pate, B. H. *Science* **2008**, *320*, 924.

(59) Scherer, N. F.; Zewail, A. H. *J. Chem. Phys.* **1987**, *87*, 97.

(60) Khundkar, L. R.; Knee, K. L.; Zewail, A. H. *J. Chem. Phys.* **1987**, *87*, 77.

(61) Scherer, N. F.; Sipes, C.; Bernstein, R. B.; Zewail, A. H. *J. Chem. Phys.* **1990**, *92*, 5239.

(62) Ionov, S. I.; Brucker, G. A.; Jaques, C.; Valachovic, L.; Wittig, C. *J. Chem. Phys.* **1993**, *99*, 6553.

(63) Ionov, S. I.; Brucker, G. A.; Jaques, C.; Chen, Y.; Wittig, C. *J. Chem. Phys.* **1993**, *99*, 3420.

(64) Kirmse, B.; Abel, B.; Schwarzer, D.; Grebenshchikov, S. Yu.; Schinke, R. *J. Phys. Chem. A* **2000**, *104*, 10374.

(65) Kim, S. K.; Guo, J.; Baskin, J. S.; Zewail, A. H. *J. Phys. Chem.* **1996**, *100*, 9202.

(66) Polik, W. F.; Guyer, D. R.; Moore, C. B. *J. Chem. Phys.* **1990**, *92*, 3453.

(67) Choi, Y. S.; Moore, C. B. *J. Chem. Phys.* **1992**, *97*, 1010.

(68) Tobison, J. D.; Dunlap, J. R.; Rohlfing, E. A. *J. Chem. Phys.* **1995**, *103*, 1448.

(69) Stöck, C.; Li, X.; Keller, H.-M.; Schinke, R.; Temps, F. *J. Chem. Phys.* **1997**, *106*, 5333.

(70) Dertinger, S.; Geers, A.; Kappert, J.; Weibrecht, J.; Temps, F. *Faraday Discuss. Chem. Soc.* **1995**, *102*, 31.

(71) Dutton, G.; Barnes, R. J.; Sinha, A. *J. Chem. Phys.* **1999**, *111*, 4976.

(72) Callegari, A.; Rebstein, J.; Jost, R.; Rizzo, T. R. *J. Chem. Phys.* **1999**, *111*, 7359.

(73) Foy, B. R.; Casassa, M. P.; Stephenson, J. C.; King, D. S. *J. Chem. Phys.* **1989**, *90*, 7037.

(74) Reiche, F.; Abel, B.; Beck, R. D.; Rizzo, T. R. *J. Chem. Phys.* **2002**, *116*, 10267.

(75) Bunker, D. L. *J. Chem. Phys.* **1962**, *37*, 393.
(76) Bunker, D. L. *J. Chem. Phys.* **1964**, *40*, 1946.
(77) Bunker, D. L.; Hase, W. L. *J. Chem. Phys.* **1973**, *59*, 4621.
(78) (a) Hase, W. L.; Feng, D. F. *J. Chem. Phys.* **1974**, *61*, 4690. (b) Hase, W. L.; Feng, D. F. *J. Chem. Phys.* **1976**, *64*, 651.
(79) Sloane, C. S.; Hase, W. L. *J. Chem. Phys.* **1977**, *66*, 1523.
(80) Wolf, R. J.; Hase, W. L. *J. Chem. Phys.* **1980**, *72*, 316.
(81) Wolf, R. J.; Hase, W. L. *J. Chem. Phys.* **1980**, *73*, 3779.
(82) Hase, W. L.; Wolf, R. J. *J. Chem. Phys.* **1981**, *75*, 3809.
(83) Hase, W. L.; Duchovic, R. J.; Swamy, K. N; Wolf, R. J. *J. Chem. Phys.* **1984**, *80*, 714.
(84) Hase, W. L.; Wolf, R. J.; Sloane, C. S. *J. Chem. Phys.* **1979**, *70*, 2911.
(85) Hase, W. L.; Buckowski, D. G. *J. Comput. Chem.* **1982**, *3*, 335.
(86) Hu, X.; Hase, W. L. *J. Chem. Phys.* **1991**, *95*, 8073.
(87) Vande Linde, S. R.; Hase, W. L. *J. Chem. Phys.* **1990**, *93*, 7962.
(88) Peslherbe, G. H.; Wang, H.; Hase, W. L. *J. Chem. Phys.* **1995**, *102*, 5626.
(89) Doubleday, C., Jr.; Bolton, K.; Peslherbe, G. H.; Hase, W. L. *J. Am. Chem. Soc.* **1996**, *118*, 9922.
(90) Lourderaj, U.; Park, K.; Hase, W. L. *Int. Rev. Phys. Chem.* **2008**, *27*, 1.
(91) Dobbyn, A. J.; Stumpf, M.; Keller, H.-M.; Schinke, R. *J. Chem. Phys.* **1996**, *104*, 8357.
(92) Sewell, T. D.; Schranz, H. W.; Thompson, D. L.; Raff, L. M. *J. Chem. Phys.* **1991**, *95*, 8089.
(93) Shalashilin, D. V.; Thompson, D. L. *J. Chem. Phys.* **1997**, *107*, 6204.
(94) Wales, D. J.; Doye, J. P. K.; Miller, M. A.; Mortensen, P. N.; Walsh, T. R. *Adv. Chem. Phys.* **2000**, *115*, 1.
(95) Carpenter, B. K. *Annu. Rev. Phys. Chem.* **2005**, *56*, 57.
(96) Oxtoby, D. W.; Rice, S. A. *J. Chem. Phys.* **1976**, *65*, 1676.
(97) Jaffé, C.; Brumer, P. *J. Chem. Phys.* **1980**, *73*, 5646.
(98) Hose, G.; Taylor, H. A. *J. Chem. Phys.* **1982**, *76*, 5356.
(99) Sibert, E. L., III; Reinhardt, W. P.; Hynes, J. T. *J. Chem. Phys.* **1982**, *77*, 3583.
(100) (a) Jaffé, C.; Reinhardt, W. P. *J. Chem. Phys.* **1982**, *77*, 5191. (b) Shirts, R. B.; Reinhardt, W. P. *J. Chem. Phys.* **1982**, *77*, 5204.
(101) Brickmann, J.; Pfeiffer, R.; Schmidt, P. C. *Ber. Bunsen-Ges. Phys. Chem.* **1984**, *88*, 382.
(102) Gutzwiller, M. C. *Chaos in Classical and Quantum Mechanics*; Springer: New York, 1990.
(103) Lichtenberg, A. J.; Lieberman, M. A. *Regular and Chaotic Dynamics*; 2nd Ed.; Springer: New York, 1992.
(104) Ezra, G. S. In *Advances in Classical Trajectory Simulations*, Vol.1; Hase, W. L., Ed.; JAI: London, 1992; Vol *1*.
(105) Davis, M. J. *Int. Rev. Phys. Chem.* **1995**, *14*, 15.
(106) Keshavamurthy, S.; Ezra, G. S. *J. Chem. Phys.* **1997**, *107*, 156.
(107) Marcus, R. A. *Faraday Discuss. Chem. Soc.* **1973**, *55*, 34.
(108) Miller, W. H. *Adv. Chem. Phys.* **1974**, *25*, 69.
(109) Lawton, R. T.; Child, M. S. *Mol. Phys.* **1981**, *44*, 709.
(110) Heller, E. J. *Faraday Discuss. Chem. Soc.* **1983**, *75*, 141.
(111) Swamy, K. N.; Hase, W. L.; Garrett, B. C.; McCurdy, C. W.; McNutt, J. F. *J. Phys. Chem.* **1986**, *90*, 3517.
(112) Brumer, P.; Shapiro, M. *Adv. Chem. Phys.* **1988**, *70*, 365.
(113) Wyatt, R. E.; Iung, C; Leforestier, C. *J. Chem. Phys.* **1992**, *97*, 3477.
(114) Hase, W. L. *J. Phys. Chem.* **1982**, *86*, 2873.
(115) Waite, B. A.; Miller, W. H. *J. Chem. Phys.* **1980**, *73*, 3713.
(116) (a) Miller, W. H. *Chem. Rev.* **1987**, *87*, 19. (b) Hase, W. L.; Cho, S.-W.; Lu, D.-H.; Swamy, K. N. *Chem. Phys.* **1989**, *139*, 1.
(117) Stumpf, M.; Dobbyn, A. J.; Keller, H.-M; Hase, W. L.; Schinke, R. *J. Chem. Phys.* **1995**, *102*, 5867.
(118) Wang, D.; Bowman, J. M. *Chem. Phys. Lett.* **1995**, *235*, 277.
(119) Stumpf, M.; Dobbyn, A. J.; Mordaunt, D. H.; Keller, H.-M; Flöthmann, H.; Schinke, R. *Faraday Dissuss. Chem. Soc.* **1995**, *102*, 193.
(120) Keller, H.-M.; Flöthmann, H.; Dobbyn, A. J.; Schinke, R.; Werner, H.-J.; Bauer, C.; Rosmus, P. *J. Chem. Phys.* **1996**, *105*, 4983.
(121) Keller, H.-M.; Schröder, T.; Stumpf, M.; Stöck, C.; Temps, F.; Schinke, R.; Werner, H.-J; Bauer, C; Rosmus, P. *J. Chem. Phys.* **1997**, *106*, 5359.
(122) Weiss, J.; Hauschildt, J.; Schinke, R.; Hann, O.; Skokov, S.; Bowman, J. M.; Mandelshtam, V. A.; Peterson, K. A. *J. Chem. Phys.* **2001**, *115*, 8880.
(123) Gray, S. K.; Goldfield, E. M. *J. Phys. Chem. A* **2001**, *105*, 2634.
(124) Skokov, S.; Bowman, J. M. *J. Chem. Phys.* **1999**, *110*, 9789.
(125) Vayner, G.; Addepalli, S. V.; Song, K.; Hase, W. L. *J. Chem. Phys.* **2006**, *125*, 014317.
(126) López, J. G.; Vayner, G.; Lourderaj, U.; Addepalli, S. V.; Kato, S.; de Jong, W. A.; Windus, T. L.; Hase, W. L. *J. Am. Chem. Soc.* **2007**, *129*, 9976.
(127) Debbert, S. L.; Carpenter, B. K.; Hrovat, D. A.; Borden, W. T. *J. Am. Chem. Soc.* **2002**, *124*, 7896.
(128) Ammal, S. C.; Yamataka, H.; Aida, M.; Dupuis, M. *Science* **2003**, *299*, 1555.
(129) Townsend, D.; Lajankar, S. A.; Lee, S. K.; Chambreau, S. D.; Suits, A. G.; Zhang, X.; Rheinecker, J.; Harding, L. B.; Bowman, J. M. *Science* **2004**, *306*, 1158.
(130) Lahankar, S. A.; Chambreau, S. D; Townsend, D.; Suits, F.; Farnum, J.; Zhang, X.; Bowman, J. M.; Suits, A. G. *J. Chem. Phys.* **2006**, *125*, 044303.
(131) Houston, P. L.; Kable, S. H. *Proc. Natl. Acad. Sci. U.S.A.* **2006**, *103*, 16079.
(132) Non-RRKM dynamics for trimethylene is also observed for simulations based on an analytic PES; see: Hrovat, D. A.; Fang, S.; Borden, W. T.; Carpenter, B. K. *J. Am. Chem. Soc.* **1997**, *119*, 5253.
(133) (a) Sun, L; Hase, W. L.; Song, K *J. Am. Chem. Soc.* **2001**, *123*, 5753. (b) Cheon, S.; Song, K.; Hase, W. L. *J. Mol. Struct.: THEOCHEM* **2006**, *771*, 27.
(134) Doubleday, C.; Li, G.; Hase, W. L. *Phys. Chem. Chem. Phys.* **2002**, *4*, 304.
(135) Mann, D. J.; Hase, W. L. *J. Am. Chem. Soc.* **2002**, *124*, 3208.
(136) Sun, L.; Song, K.; Hase, W. L. *Science* **2002**, *124*, 3208.
(137) Sun, L.; Chang, E.; Song, K.; Hase, W. L. *Can. J. Chem.* **2004**, *82*, 891.
(138) Marcy, T. P.; Diaz, R. R.; Heard, D.; Leone, S. R.; Harding, L. B.; Klippenstein, S. J. *J. Phys. Chem. A* **2001**, *105*, 8361.
(139) Mikosh, J.; Trippel, S.; Eichhorn, C.; Otto, R.; Lourderaj, U.; Zhang, J. X.; Hase, W. L.; Weidemüller, M.; Wester, R. *Science* **2008**, *319*, 183.
(140) Slater, N. B.; *Theory of Unimolecular Reactions*; Cornell University Press: Ithaca, NY, 1959.
(141) Miller, W. H. *J. Chem. Phys.* **1976**, *65*, 2216.
(142) Doll, J. D. *J. Chem. Phys.* **1980**, *73*, 2760.
(143) Rice, O. K. *Z. Phys. Chem. B* 1930, *7*, 226; quoted by Kassel, L. S. *Kinetics of Homogeneous Reactions*; Chemical Catalog: New York, 1932.
(144) (a) Fermi, E.; Pasta, J.; Ulam, S. *Studies on Non-Linear Problems I*; Los Alamos Scientific Laboratory: Los Alamos, NM, 1955. (b) Dauxios, T. *Physics Today* **2008**, 55.
(145) (a) Sloane, C. S.; Hase, W. L. *Faraday Discuss. Chem. Soc.* **1977**, *62*, 210. (b) Hase, W. L.; Mrowka, G.; Brudzynski, R. J.; Sloane, C. S. *J. Chem. Phys.* **1978**, *69*, 3548.
(146) Bach, A.; Hostettler, J. M.; Chen, P. *J. Chem. Phys.* **2005**, *123*, 021101.
(147) Bach, A.; Hostettler, J. M.; Chen, P. *J. Chem. Phys.* **2006**, *125*, 024304.
(148) Gilbert, T.; Grebner, T. L.; Fischer, I.; Chen, P. *J. Chem. Phys.* **1999**, *110*, 5485.
(149) Amaral, G.; Xu, K. S.; Zhang, J. S. *J. Chem. Phys.* **2001**, *114*, 5164.
(150) (a) Hase, W. L.; Schlegel, H. B. *J. Phys. Chem.* **1982**, *86*, 3901. (b) Hase, W. L.; Schlegel, H. B.; Bolbyshev, V.; Page, M. *J. Phys. Chem.* **1996**, *100*, 5354.
(151) Rabinovitch, B. S.; Setser, D. W. *Adv. Photochem.* **1964**, *3*, 1.
(152) Forst, W. *Theory of Unimolecular Reactions*; Academic Press: New York, 1973.
(153) Robinson, P. J.; Holbrook, K. A. *Unimolecular Reactions*; Wiley: New York, 1972.
(154) Gilbert, R. G.; Smith, S. C. *Theory of Unimolecular and Recombination Reactions*; Blackwell: London, 1990.
(155) Marcus, R. A.; Hase, W. L.; Swamy, K. N. *J. Phys. Chem.* **1984**, *88*, 6717.
(156) Lu, D.-H.; Hase, W. L. *J. Phys. Chem.* **1989**, *93*, 1681.
(157) Miller, W. H. *J. Phys. Chem.* **1988**, *92*, 4261.
(158) Moiseyev, N.; Wyatt, R. E. *Chem. Phys. Lett.* **1986**, *132*, 396.
(159) Polik, W. F.; Guyer, D. R.; Miller, W. H.; Moore, C. B. *J. Chem. Phys.* **1990**, *92*, 3471.
(160) Levine, R. D. *Adv. Chem. Phys.* **1987**, *70*, 53.
(161) Porter, C. E.; Thomas, R. G. *Phys. Rev.* **1956**, *104*, 483.
(162) Other distributions of $P(k)$ are considered in Lu, D.-H; Hase, W. L. *J. Chem. Phys.* **1989**, *90*, 1557. A generalization of the Porter−Thomas distribution and a random matrix/transition-state theory model are discussed in Hernandez, R.; Miller, W. H.; Moore, C. B.; Polik, W. F. *J. Chem. Phys.* **1993**, *99*, 950.
(163) Green, W. H., Jr.; Moore, C. B.; Polik, W. F. *Annu. Rev. Phys. Chem.* **1992**, *43*, 591.
(164) Miller, W. H.; Hernandez, R.; Moore, C. B.; Polik, W. F. *J. Chem. Phys.* **1990**, *93*, 5657.
(165) (a) Song, K.; Sun, L.; Hase, W. L.; Grebenshchikov, S. Yu.; Schinke, R. *J. Phys. Chem. A* **2002**, *106*, 8339. (b) Song, K.; Hase, W. L. *J. Phys. Chem. A* **1998**, *102*, 1292.
(166) Hippler, H.; Krasteva, N.; Striebel, F. *Phys. Chem. Chem. Phys.* **2004**, *6*, 3383.
(167) Miller, W. H. *J. Phys. Chem.* **1995**, *99*, 12387.
(168) Lovejoy, E. R.; Kim, S. K.; Moore, C. B. *Science* **1992**, *256*, 1541.

(169) Ionov, S. I.; Davis, H. F.; Mikhaylichenko, K.; Lalachovic, L.; Beaudet, R. A.; Wittig, C. *J. Chem. Phys.* **1994**, *109*, 4809.
(170) Leu, G.-H.; Huang, C.-L.; Lee, S.-H.; Lee, Y.-C.; Chen, I.-C. *J. Chem. Phys.* **1998**, *109*, 9340.
(171) King, R. A.; Allen, W. D.; Schaefer, H. F., III. *J. Chem. Phys.* **2000**, *112*, 5585.
(172) Gezelter, J. D.; Miller, W. H. *J. Chem. Phys.* **1996**, *104*, 3546.
(173) Grebenshchikov, S. Yu.; Beck, C.; Flöthmann, H.; Schinke, R.; Kato, S. *J. Chem. Phys.* **1999**, *111*, 619.
(174) Marcus, R. A. *Science* **1992**, *256*, 1523.
(175) Zhu, L.; Hase, W. L. *Chem. Phys. Lett.* **1990**, *175*, 117.
(176) Aubanel, E. E.; Wardlaw, D. M.; Zhu, L.; Hase, W. L. *Int. Rev. Phys. Chem.* **1991**, *10*, 249.
(177) Hase, W. L. *Acc. Chem. Res.* **1998**, *62*, 659.
(178) Schlier, Ch. G. *Mol. Phys.* **1987**, *62*, 1009.
(179) Brass, O.; Schlier, Ch. *J. Chem. Phys.* **1988**, *88*, 936.
(180) (a) North, S. W.; Hall, G. E. *J. Chem. Phys.* **1997**, *106*, 60. (b) North, S. W.; Hall, G. E. *Ber. Bunsen-Ges. Phys. Chem.* **1997**, *101*, 459.
(181) Grebenshchikov, S. Y.; Flöthmann, H.; Schinke, R.; Bezel, I.; Wittig, C; Kato, S. *Chem. Phys. Lett.* **1998**, *285*, 410.
(182) Peslherbe, G. H.; Hase, W. L. *J. Chem. Phys.* **1994**, *101*, 8535.
(183) Song, K.; Hase, W. L. *J. Chem. Phys.* **1999**, *110*, 6198.
(184) Abramson, E.; Field, R. W.; Imre, D.; Innes, K. K.; Kinsey, J. L. *J. Chem. Phys.* **1985**, *83*, 453.
(185) Wagner, A. F.; Kiefer, J. H.; Kumaran, S. S. In *Twenty-Fourth Symposium on Combustion*; The Combustion Institute: Pittsburgh, PA, 1992; pp 613−619.
(186) Bhuiyan, L. B.; Hase, W. L. *J. Chem. Phys.* **1983**, *78*, 5052.
(187) Peslherbe, G. H.; Wang, H.; Hase, W. L. *J. Chem. Phys.* **1995**, *102*, 5626.
(188) Troe, *J. Chem. Phys.* **1995**, *190*, 381.
(189) Yao, L.; Mebel, A. M.; Lu, H. F.; Neusser, H. J.; Lin, S. H. *J. Phys. Chem. A* **2007**, *111*, 6722.
(190) Hu, X.; Hase, W. L. *J. Chem. Phys.* **1991**, *95*, 8073.
(191) Lourderaj, U.; McAfee, J. L.; Hase, W. L. *J. Chem. Phys.* **2008**, *129*, 094701.
(192) Vande Linde, S. R.; Hase, W. L. *J. Chem. Phys.* **1990**, *93*, 7962.
(193) Li, C.; Ross, P.; Szulejo, J. E.; McMahon, T. B. *J. Am. Chem. Soc.* **1996**, *118*, 9360.
(194) Mikosch, J.; Otto, R.; Trippel, S.; Eichhorn, C.; Weidemüller, M.; Wester, R. *J. Phys. Chem. A.* **2008**, 112.
(195) Wester, R; Bragg, A. E.; Davis, A. V.; Neumark, D. M. *J. Chem. Phys.* **2003**, *119*, 10032.
(196) Tonner, D. S.; McMahon, T. B. *J. Am. Chem. Soc.* **2000**, *122*, 8783.
(197) Borchardt, D. B.; Bauer, S. H. *J. Chem. Phys.* **1986**, *85*, 4980.
(198) Lee, C. Y.; Pate, B. H. *J. Chem. Phys.* **1997**, *107*, 10430.
(199) McWhorter, D. A.; Hudspeth, E.; Pate, B. H. *J. Chem. Phys.* **1999**, *110*, 2000.
(200) Baer, T.; Potts, A. R. *J. Phys. Chem. A* **2000**, *104*, 9397.
(201) (a) Dian, B. C.; Longarte, A.; Zwier, T. S. *Science* **2002**, *296*, 2369. (b) Evans, D. A.; Wales, D. J.; Dian, D. C.; Zwier, T. S. *J. Chem. Phys.* **2004**, *120*, 148.
(202) Schanz, R.; Botan, V.; Hamm, P. *J. Chem. Phys.* **2005**, *122*, 044509.
(203) (a) Northrup, S. H.; Hynes, J. T. *J. Chem. Phys.* **1980**, *73*, 2700. (b) Nordholm, S. *Chem. Phys.* **1989**, *137*, 109.
(204) (a) Leitner, D. M.; Wolynes, P. G. *Chem. Phys. Lett.* **1997**, *280*, 411. (b) Gruebele, M.; Wolynes, P. G. *Acc. Chem. Res.* **2004**, *37*, 261.
(205) Weston, R. E., Jr.; Barker, J. R. *J. Phys. Chem. A* **2006**, *110*, 7888.
(206) Osterheld, T. H.; Brauman, J. I. *J. Am. Chem. Soc.* **1993**, *115*, 10311.
(207) Nummela, J. A.; Carpenter, B. K. *J. Am. Chem. Soc.* **2002**, *124*, 8512.
(208) Fenn, P. T.; Chen, Y.-J; Stimson, S.; Ng, C. Y. *J. Phys. Chem. A* **1997**, *101*, 6513.
(209) Martínez-Núñez, E.; Vázquez, S. A.; Marques, J. M. C. *J. Chem. Phys.* **2004**, *121*, 2571.
(210) Fukui, K. *J. Phys. Chem.* **1970**, *74*, 4161.
(211) (a) Bolton, K.; Hase, W. L.; Peslherbe, G. H. In *Multidimensional Molecular Dynamics Methods*; Thompson, D. L. Ed.; World Scientific: London, 1998; p 143. (b) Sun, L.; Hase, W. L. *Rev Comput. Chem.* **2003**, *19*, 79.
(212) Blanksby, S. J.; Ellison, G. B.; Bierbaum, B. V.; Kato, S. *J. Am. Chem. Soc.* **2002**, *124*, 3196.

JP806659F